Liquid Crystals
Publication details, including instructions for authors and subscription information:
http://www.informaworld.com/smpp/title~content=t713926090

Invited Article. X-ray diffraction by mesomorphic comb-like polymers

P. Davidson[a]; A. M. Levelut[a]
[a] Laboratoire de Physique des Solides, associé au CNRS, Batiment 510, Université Paris XI, Orsay, Cédex, France

To cite this Article Davidson, P. and Levelut, A. M.(1992) 'Invited Article. X-ray diffraction by mesomorphic comb-like polymers', Liquid Crystals, 11: 4, 469 — 517
To link to this Article: DOI: 10.1080/02678299208029006
URL: http://dx.doi.org/10.1080/02678299208029006

LIQUID CRYSTALS, 1992, VOL. 11, NO. 4, 469–517

Invited Article

X-ray diffraction by mesomorphic comb-like polymers

by P. DAVIDSON* and A. M. LEVELUT

Laboratoire de Physique des Solides, associé au CNRS, Batiment 510, Université Paris XI, 91405 Orsay Cédex, France

(*Received 27 June 1991*)

This article presents a survey of the literature on X-ray diffraction by mesomorphic comb-like polymers. Special emphasis is placed upon two points: it is often possible to study the localization of the backbone in the smectic phases by considering the intensities of the Bragg reflections from the layers. It is also possible to observe different kinds of short range order and localized defects through their contribution to the X-ray diffuse scattering. For instance, the average S_A structure may be affected by layer undulations or disturbed by edge dislocations. By examining the many X-ray diffraction studies already published, it can be shown that the backbones have an ambiguous influence upon the molecular organization. They sometimes tend, for entropic reasons, to lessen the positional long range order or to create defects, whereas they sometimes promote short range order because they induce correlations among the mesogenic cores chemically linked to them.

1. Introduction

Mesomorphic side chain polymers have been known for a long time [1] and by applying the flexible spacer concept [2] a large number of them have been synthesized [3]. They combine the properties of liquid crystals as anisotropic fluids with the mechanical properties of polymers, in particular they present a glass transition at T_g below which the molecular organization may be frozen in. These compounds have mainly attracted interest because of possible applications in the fields of non-linear optics, optical storage and electro-optic displays [3]. Thus, chemists have devised a large variety of such polymers in order to tailor them for these specific applications. Among all of these types of mesomorphic side chain polymers, we shall only consider the classical scheme of thermotropic, comb-like polymers (see figure 1). This excludes

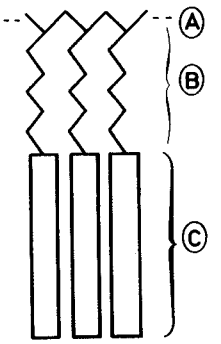

Figure 1. Schematic representation of a mesomorphic comb-like polymer. A, Backbone; B, flexible spacer; C, mesogenic core.

*Author for correspondence

0267–8292/92 $3·00 1992 Taylor & Francis Ltd.

the cases of lyotropic polymers, mesomorphic networks, mixtures, copolymers, combined polymers, discotic or phasmidic polymers, etc. This article is also meant to summarize and articulate eight papers and a Ph.D. thesis published from 1984 to 1991 [4–12]. The experimental set-ups will not be described here since they are in the original papers and since they are commonly employed in X-ray laboratories.

The polymorphism of mesomorphic side chain polymers is usually studied by differential scanning calorimetry, optical microscopy with polarized light and X-ray diffraction [13]. Indeed, numerous studies have appeared in which X-ray diffraction is used as a tool useful to check the nature of the mesophases displayed by a given series of compounds. In many other studies X-ray diffraction also helps to determine the alignment direction of the mesogenic cores or sometimes that of the backbones under the influence of an external field such as a magnetic field or under the influence of a rheological process such as fibre drawing. X-ray diffraction studies which go beyond these simple characterization goals are less frequent and may easily be summarized as follows.

Several papers deal with the mean molecular packing in the smectic (S_A, S_B. S_C, S_E...) phases and in particular with the relation between the molecular length l and the smectic periodicity d [4–6, 10, 14–40].

A German team has tried, in addition, to exploit the relationships between the crystalline structures of samples aligned either by fibre drawing or by a magnetic field and those of the corresponding mesophases [41–43]. These authors have also studied the effects of thermal history upon the molecular packing.

Russian scientists have shown that it is possible to infer the electron density profile along the normal to the layers from the intensity of the reflections from the smectic layers. They have also studied the influence of temperature and spacer length on the correlation lengths of the long range order in several smectic phases [44–55]. (We comment on their results in § 2.)

The critical behaviour around several phase transitions such as S_A–N and S_C–N has been extensively studied by high resolution X-ray diffraction [56–59]. This technique has also allowed the observation of unexpected effects such as an unusual tilt angle temperature dependence in the S_C phase and anharmonicity effects in the S_A phase. (All of these results will also be briefly reviewed in § 2.)

A few studies deal with the measurements of the nematic [60] and smectic [29, 47, 61] order parameters as a function of temperature.

Short range order and defects have only been seldom considered [4, 5, 7, 10, 12, 30, 33, 36, 37, 45, 46] (see §§ 3 and 4).

At this point, it is interesting to briefly compare X-ray diffraction with other techniques. Small angle neutron scattering experiments on partially deuteriated compounds have proved to be very useful to study the backbone conformations in several mesophases (N, S_A) [62]. However this method demands large samples and the deuteriation of well chosen molecular sites. Measurements of the Bragg reflections on the layers can also be performed with neutron diffractometers but with a lower signal/noise ratio compared to that attainable with X-rays. Nevertheless, these measurements would still be instructive because nuclear scattering lengths which govern neutron scattering are different from atomic scattering factors of X-rays and therefore additional information would be obtained in this way.

Electron microscopy has been performed on thin films of mesomorphic polymers [63–69] revealing interesting packing details as well as defects. For instance, smectic layer undulations with a very large period (a few 100 Å) have been detected. Edge

dislocations disturbing the smectic ordering have also been observed directly. However, these experiments are sophisticated because the sample must be prepared carefully and the signal treatment is quite elaborate. In addition, the molecular organization in thin films often differs from that of the bulk.

Light scattering experiments should give information about fluctuations on the length scale of a micron (compared to 1–1000 Å with X-rays or neutrons). It has seldom been used in such systems [46, 51] and only to determine the orientation of domains with respect to the average director.

Dynamic techniques such as dielectric spectroscopy [70], ultrasound propagation [71–73] or nuclear magnetic resonance [74–81] have also been employed to study such systems. These techniques are quite complementary to the X-ray diffraction methods which generally cannot distinguish between static and dynamic phenomena. Dielectric spectroscopy essentially gives information about the motion of the different molecular moieties. Usually both the frequency and activation energy for each movement may be obtained. Ultrasound propagation allows us to measure the values of the elastic constants as a function of frequency. The critical behaviour around phase transitions can also be studied with this technique. NMR has so far been the most extensively used dynamic technique since it can give many kinds of information: local conformations and order parameters of the different moieties, molecular movements with their relaxation times and activation energies as well as estimates of the elastic constants by transient methods.

This article is divided into three parts. The first deals with the mean structure, i.e. the long range order in the different mesophases, particularly in the S_A and S_B phases. The smectic pretransitional fluctuations in the nematic phase are also discussed briefly in this section.

The second deals with the short range order which affects these mean structures. By short range order, we mean the fluctuations of symmetries lower than that of the mean structure and extending over finite correlation lengths.

Finally, the third deals with localized structural defects, such as dislocations.

In the following, in order to avoid any ambiguity, we shall sometimes refer to a polymeric mesophase as that displayed by comb-like polymers (for instance, a polymeric S_B phase) as opposed to a conventional mesophase for that displayed by the usual low molar mass mesogens.

2. Mean structures of the polymeric mesophases

In order to perform X-ray diffraction studies, it is more convenient to use aligned domains rather than powder samples for two reasons: the information about relative angles between structural features is often lost by powder averaging; the intensity scattered by an aligned sample lies in smaller solid angles resulting in larger signal-to-noise ratios. Such aligned domains are usually obtained either by action of a magnetic (or sometimes electric) field or by a rheological process (such as sample shearing or fibre drawing) followed by sample freezing below T_g. Though the rheological processes may be very helpful for polymers too viscous to be aligned by an external field, they should be employed cautiously because samples obtained in this way are not in thermodynamic equilibrium. For instance, the state of alignment depends upon the initial temperature of the melt from which the fibre is drawn and also upon the mesophase displayed by the melt [26]. This may lead to apparent discrepancies between the states of alignment (whether the backbones or the mesogenic cores are aligned parallel to the flow) published in the literature [4, 34]. The molecular organizations are also slightly

different in a drawn fibre and in a magnetically aligned sample. Subsequent heating of the fibre sometimes helps to recover the thermodynamic equilibrium state [4]. If the compound displays a rich polymorphism, more than one mesophase may be trapped in the freezing process (for instance in the skin and in the core of the fibre) which results in complicated X-ray diffraction patterns.

2.1. *The nematic phase*

The nematic phase has only positional liquid-like short range order and therefore the information obtained from the diffraction patterns is scarce. It essentially amounts to the evaluation of the molecular axis angular distribution function $f(\theta)$ together with the nematic order parameter $\langle P_2 \rangle = \langle 3\cos^2\theta - 1 \rangle / 2$ [60] (which seems to behave in a similar way as that of the conventional nematic phase) and often also to the estimation of an apparent length for the side chains [4, 31, 34, 52, 56, 58, 61]. In some cases, the nematic phase exhibits strong smectic fluctuations. This allows the study of the critical behaviour around phase transitions such as S_A–N or S_C–N by high resolution X-ray diffraction [52, 56, 58]. Thus it was found that at the S_A–N transition, the pretransitional S_A fluctuations in the N phase gave rise to a diffuse scattering which can be described by a simple Ornstein–Zernike expression. These fluctuations displayed correlation lengths $\xi_{\parallel} = \xi^{\circ} t^{-\nu_{\parallel}}$ and $\xi_{\parallel} = \xi^{\circ} t^{-\nu_{\perp}}$ where t is the reduced temperature, with exponents $\nu_{\parallel}$ and $\nu_{\perp}$ comparable to those of conventional liquid crystals. According to the authors of [58] these facts suggest that the nature and symmetry of the forces between mesogens are not changed in the presence of the backbones. However, the influence of the backbones was to increase the values of the bare correlation lengths $\xi^{\circ}_{\parallel}$ and $\xi^{\circ}_{\perp}$ which was accounted for by the propagation of the nearest neighbour interactions via the backbone. A similar study was performed upon the S_C–N transition [56]: it appeared that the pretransitional fluctuations could be described by the Chen–Lubensky mean field model devised for conventional mesogens and that the only influence of the backbones was to lessen the divergence of the correlation lengths in the vicinity of the phase transition. To summarize these studies, it seems that the polymer backbones do not influence the nature and symmetry of the forces between mesogens. The backbones rather enhance the short range local order by propagating nearest neighbour interactions but they may also eventually lessen the long range order due to their finite size.

Other types of short range order which will be described at length in § 3 can also affect the polymeric nematic phase. Such short range orders affect the mean smectic structures too but with larger correlation lengths than in the nematic phase.

2.2. *The S_A phase*

2.2.1. *The different structural approaches*

The S_A phase has one dimensional long range order: the mesogens are stacked in layers and are, on average, perpendicular to these layers. Moreover, a liquid-like order prevails within the layers. Therefore, the S_A phase can be described as one dimensional stack of liquid layers. The X-ray diffraction pattern (see figure 2) generally consists of a few (usually, only one or two) small angle Bragg reflections from the layers and a wide angle diffuse ring [13].

In order to determine the specificity of mesomorphic comb-like polymers compared to the conventional mesogens, several approaches have been used. In one, the whole macromolecule constitutes the building block of the S_A phase. For instance, the polymer chain may be supposed to adopt a ribbon-like configuration with the pendant

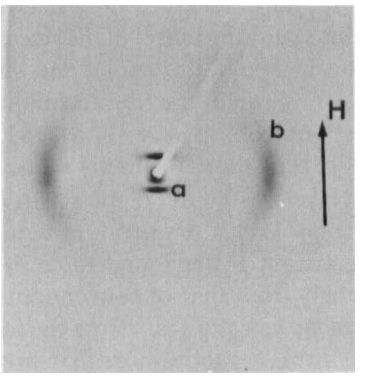

Figure 2. X-ray diffraction pattern in the S_A phase of a low molecular weight liquid crystal. a, Bragg reflections; b, wide angle diffuse ring; *H* is the magnetic field direction.

groups hanging on the same side of the backbone [14–18]. Subsequent packing of these ribbons results in the formation of the S_A phase [15, 16]. (The same idea was also applied to the description of the S_E phase [14, 17, 18].) From a similar point of view [41], the macromolecules form elliptical bodies with the elongated backbones in the centre and the mesogenic cores hanging from each side. Then these decorrelated bodies build up the S_A phase. In both cases, the backbones should display a strongly elongated conformation in a direction perpendicular to the director which was not observed in the small angle neutron scattering experiments reported so far [62]. In another approach, several teams [29, 47, 61] have measured the intensity of the first order reflection on the smectic layers versus temperature. This intensity represents a combination of the structure factor with the smectic order parameter. The following interesting effect was observed: the intensity first increases slightly with increasing temperature until it drops, as usual, in the vicinity of the S_A–N or S_A–I phase transitions. The first intensity increase was explained by admitting that the smectic ordering improves with temperature due to the annealing of defects. Nevertheless, the structure factor may also depend on temperature, all the more since the localization of the backbone may not follow that of the mesogenic cores as a function of temperature.

A more detailed approach consists of studying the Bragg reflection profiles with the help of high resolution X-ray diffraction techniques. It was found that the smectic ordering in the polymeric S_A phase, is not truly long range (actually, this applies to all S_A phases since the one dimensional long range order is destroyed by fluctuations at finite temperatures [82]) but rather extends on a length scale of about 1000 Å [49, 53, 54, 56, 58] (this value varies largely with thermal history, compound, spacer length, etc). This order of magnitude implies that the Bragg reflections will be resolution limited in the usual low resolution X-ray diffraction experiments. The correlation length increases with temperature; this was also interpreted by the annealing of defects. The influence of the spacer length on the smectic correlation length has also been studied systematically [49, 53, 54]: it appears that this correlation length increases with increasing spacer length, i.e. with decreasing backbone–mesogenic core coupling strength. Moreover, an X-ray small angle scattering intensity was detected for comb-like polymers which had no spacers [44]. This observation could be explained by the existence of heterogeneities of length scale of about 1000 Å. Such X-ray small angle scattering has never been reported for pure comb-like polymers with long enough

spacers. This observation supports the preceding conclusion. To summarize these studies, it can be said that this saturation effect of the smectic correlation length reflects the influence of the backbones, though its detailed mechanism is not understood yet.

Still using high resolution X-ray diffraction techniques Nachaliel *et al.* [59], by inspecting the Bragg reflection profiles, have shown the existence of anharmonicity effects very close to the S_A–N transition. From fits of the experimental profiles of the reflections from the smectic layers, estimates of the elastic constants B for compression of the layers and K_1 for splay versus temperature could be obtained. The critical exponent ϕ of the elastic constant B was found to be in agreement with theoretical predictions but differs strongly from that of conventional liquid crystals.

From a different point of view, we can also note the fact that the X-ray diffraction patterns of many polymeric S_A phases show more than one (sometimes up to six) order of reflection from the layers and that the first order is not necessarily the strongest. (The fact that several orders of reflection can be detected simultaneously in a fixed sample experiment shows that an appreciable mosaicity usually exists in the sample.) Such behaviour is very different to that of conventional S_A phases for which according to de Gennes' model [82], the projection of the electron density along the director is usually described by a single sinusoidal function.

Russian teams [46, 48–51, 53, 54] first exploited this situation by postulating an electron density profile made of step functions each representing a part of the molecule (backbone, spacer, mesogenic core). By Fourier transforming this profile, the experimental intensities of reflection can be accounted for by varying the parameters of this model: position, width and height of each step function. The parameters obtained are usually in good agreement with molecular models. In this way, a secondary maximum of the electron density profile has been noticed and explained by the presence of the backbone. A drawback of this method comes from the large number of model parameters to be estimated, compared to the number of Bragg reflections, especially if different Debye–Waller factors or transition regions between step functions are considered.

In contrast our approach consists of measuring the intensities of the different orders of reflection from the layers and by inverse Fourier transforming of deriving the electron density profile along the normal to the layers. This method will be discussed later but we need first to explain the problem addressed better.

Since the early papers [1] about mesomorphic side chain polymers, a central issue has been the conformation of the backbone in the different phases. In many cases, small angle neutron scattering has proved so far to be the best technique to study this point [62]. However, in some cases, this can also be done using X-rays. For instance, let us consider a smectic phase: do the backbones feel the smectic field? Are they confined as flat discs, between the smectic layers (see figure 3 (*a*)) or do they keep a more or less isotropic three dimensional conformation (see figure 3 (*b*))? This question can be tackled by inspecting the electron density profile, because if it also presents a secondary maximum, in addition to the maximum due to the cores, then this maximum should come from the fact that the backbones are well-confined between sublayers of mesogenic cores.

2.2.2. *Study of the electron density profile*

We now describe our method in more detail [8, 9]: let $\rho(z)$ be the projection of the electronic density along the normal z to the layers; $\rho(z)$ can be expanded in a Fourier series. For a conventional S_A phase, $\rho(z)$ is expected to be centrosymmetric; this is not so

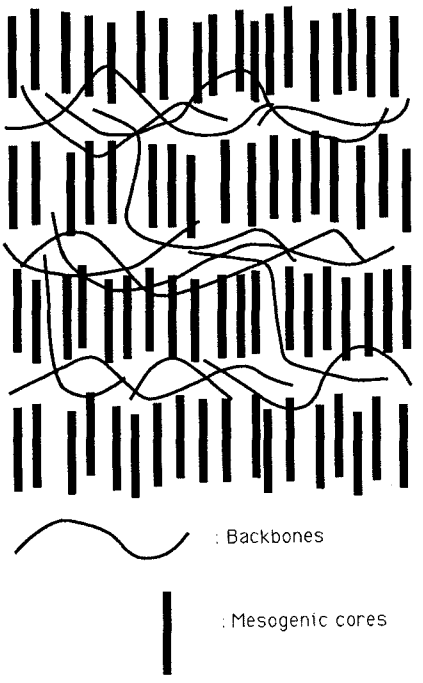

(*a*)

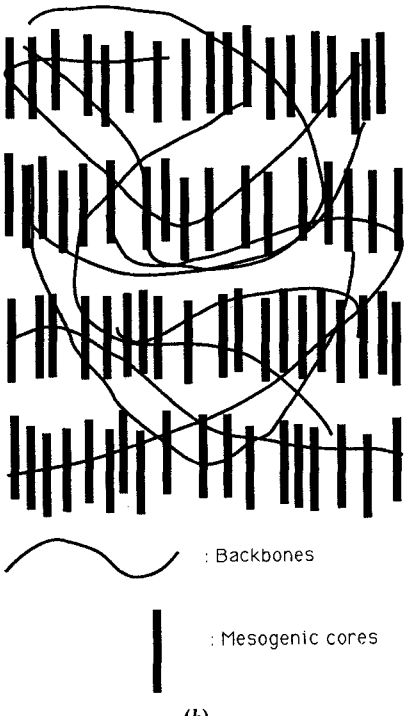

(*b*)

Figure 3. Schematic molecular organization of the polymeric smectic phases. (*a*) The backbones are confined between the sublayers of the mesogenic cores. (*b*) The backbones are not very much affected by the smectic order.

obvious for a polymeric S_A phase but it can be checked by various physical methods such as the absence of any ferroelectricity [83]. If $\rho(z)$ is centrosymmetric, then the Fourier series will only contain cosine terms so that we have

$$\rho(z)=\rho_0+\sum_n a_n \cos\frac{n2\pi z}{d},$$

where d is the smectic period, $\rho(-z)=\rho(z)$ and the a_n coefficients are real. The average value of the electronic density ρ_0 cannot be determined by X-rays with our experimental methods; we write, therefore, $\rho(z)$ to represent only the fluctuations around the average value:

$$\rho(z)=\sum_n a_n \cos\frac{n2\pi z}{d}.$$

In order to measure the intensities of the different orders of reflection, it is convenient to use either a powder or a well-aligned rotating sample. After correction of the usual technical factors (such as the Lorentz polarization factor), the experiment thus provides $|a_n|^2$ which means that the signs of the a_n coefficients remain undetermined. This is the equivalent of the well-known phase problem in classic crystallography but in a much simpler version since the a_n coefficients are real and since the problem is only one dimensional. As a consequence, all the sign combinations of the different a_n coefficients must be generated and their number grows exponentially with the number of detected reflections. Fortunately, in most cases, no more than five or six orders of reflection can be measured.

The problem is now to choose from the different sign combinations obtained which actually represents $\rho(z)$. First the sign combinations may be classified in pairs which actually represent the same profile with a phase shift of 0 or π. Then, according to the choice or the origin along the z axis and to a hypothesis about the relative electron densities of the backbones and of the mesogenic cores, half of the solutions may be ruled out. After that, the electron densities of all the different parts of the molecule may be estimated and compared to those obtained from the different sign combinations. Some kind of criterion [9] (not very accurate, though) made up from the acceptable relative values of the electron densities of the different parts of the molecule, can be used to help to discriminate between the different sign combinations. In most cases, we are left with only one possible solution, all the more easily if several compounds in the same homologous series are available.

We illustrate this method with three examples [8, 9, 84]. The first [9] deals with a series of mesomorphic side chain polysiloxanes of formula

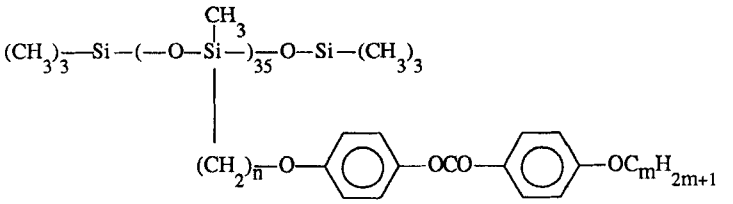

and labelled $P_{n,m}$, synthesized and characterized by Mauzac *et al.* [19]. A typical X-ray diffraction pattern in the S_A phase is presented in figure 4(*a*). Table 1 shows the amplitudes of the different orders of reflection from the smectic layers. It should be noted that for some members of this homologous series, oddly enough, the second

Table 1. Amplitudes normalized to the first, of the different orders of reflection from the smectic layers for different $P_{n,m}$ polymers; the index B refers to the smectic B phase.

	$P_{3,4}$	$P_{4,4}$	$P_{3,8}$	$P_{5,8}$	$(P_{3,8})_B$	$(P_{5,8})_B$
a_1	1	1	1	1	1	1
a_2	1·60	1·55	0·75	0·85	0·60	0·80
a_3	1·50	0·70	0·60	0·75	0·60	0·80
a_4	0·80	0	0·55	0·60	0·75	0·80
a_5	0	0	0	0·30	0	0·60

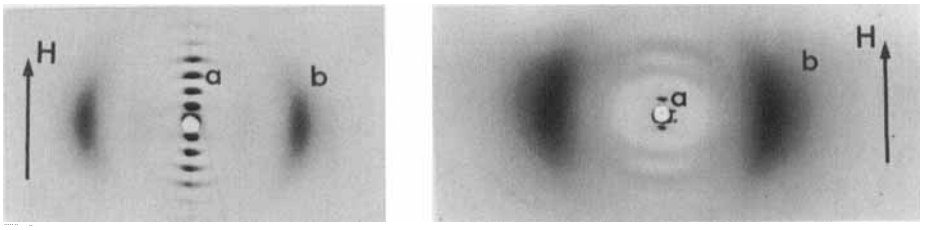

(*a*) (*b*)

Figure 4. X-ray diffraction patterns in the S_A phase of two representative polymers of the $P_{n,m}$ polysiloxane homologous series. a, Bragg reflections; b, wide angle diffuse ring; *H* is the magnetic field direction. (*a*) Polymer $P_{3,8}$; (*b*) Polymer $P_{4,1}$.

order reflection from the smectic layers is as strong or even stronger than the first. All of these polymers form a S_{A_1} ($d \approx l$) phase. Figure 5 shows the sign combinations of the a_n coefficients which represent the electron density profile $\rho(z)$ along the director for several $P_{n,m}$ polymers. These profiles display a secondary maximum due to the backbones. Such a secondary maximum makes sense if we remember that silicon atoms present in the backbones have a larger electron density than the other parts of the molecule. This implies that within a smectic layer, the backbones should be located in sublayers squeezed between adjacent sublayers of mesogenic cores (see figure 6). This case looks very much like that of figure 3(*a*); it was even described in terms of microphase separation by Russian teams [46, 48–51, 53, 54]. Looking at the electron density profiles $\rho(z)$ (see figure 5), we notice that they present a pseudoperiodicity of $d/2$ which explains why the second order reflection has an amplitude comparable to that of the first. In this particular case, the backbones are confined in sublayers from 5 to 8 Å thick along the director. By considering different members of the homologous series, it can be noticed that increasing the length of the aliphatic part of the molecule helps the backbones to resist the confinement imposed by the mesogenic cores.

Other members of the same homologous series present a completely different behaviour: $P_{4,1}$ and $P_{5,1}$ display only one appreciable order of reflection, the second order being barely detectable with a conventional apparatus (see figure 4(*b*)). For these polymers, de Gennes' model appears to apply which means that the backbones do not seem to be affected very much by the smectic field (see figure 3(*b*)). It should be noted that these polymers form S_{A_d} phase [19, 85] ($d \approx 1{\cdot}4l$) rather than S_{A_1} phases.

At this point it should be recalled that the elastic constant *B* for compression of the smectic layers also plays a role in the number of observable orders of reflection. In a

simple model [86], the intensity of the nth order of reflection will be proportional to $\exp(-4\pi^2 n^2 \langle z^2 \rangle / d^2)$ where $\langle z^2 \rangle$ is the average squared longitudinal displacement of a molecule. This term is analogous to a Debye–Waller factor for usual crystals. The $\langle z^2 \rangle$ term may indeed be evaluated by considering the thermal fluctuations of the layers calculated by de Gennes [82]; they are inversely proportional to B: $\langle z^2 \rangle \propto 1/B$. Altogether, the dependence of the intensity of the nth order of reflection goes like $\exp(-n^2/B)$. If B is large, then the Debye–Waller factor will tend to unity and several orders of reflection may be detected if the layer structure factor allows it. If B is too small, then the Debye–Waller factor will decrease the intensities of the higher orders of

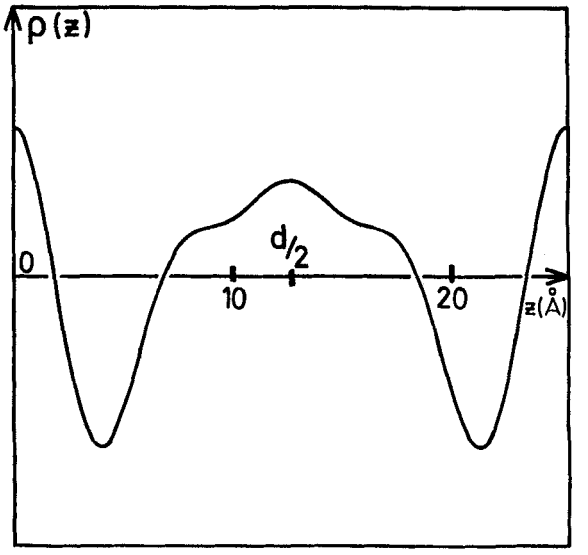

(*a*)

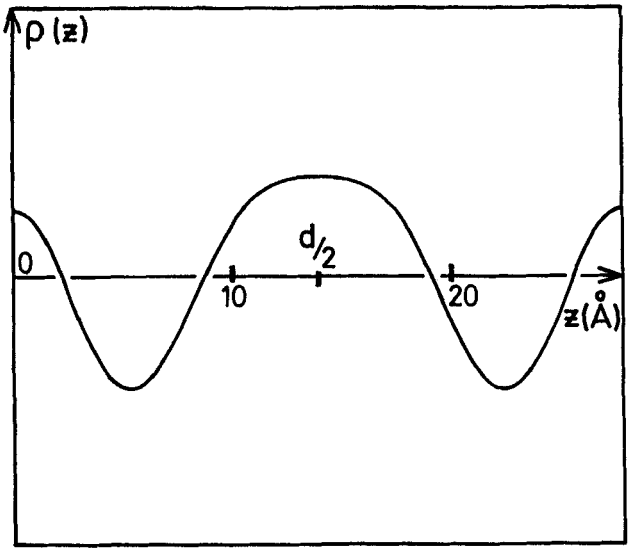

(*b*)

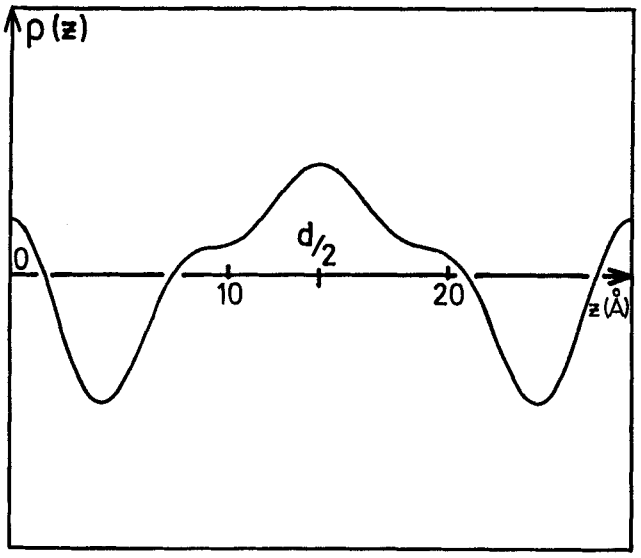

(*c*)

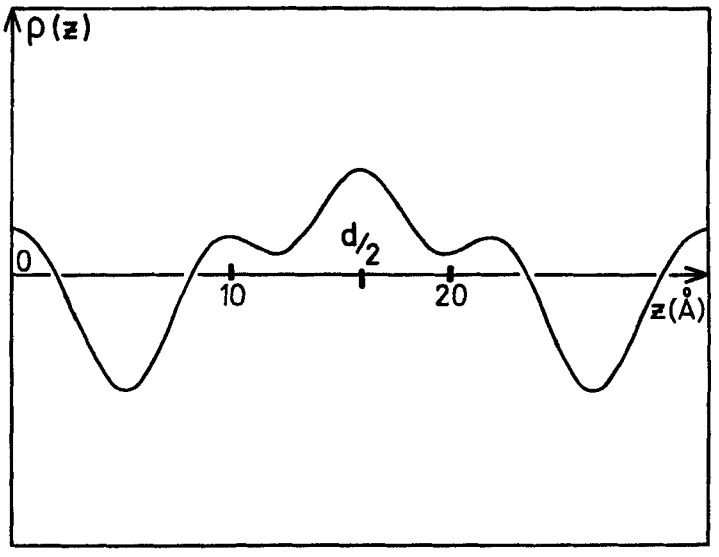

(*d*)

Figure 5. Electron density profiles $\rho(z)$ of several $P_{n,m}$ polymers in the S_A phase. (*a*) Polymer $P_{3,4}$; (*b*) Polymer $P_{4,4}$; (*c*) Polymer $P_{3,8}$; (*d*) Polymer $P_{5,8}$.

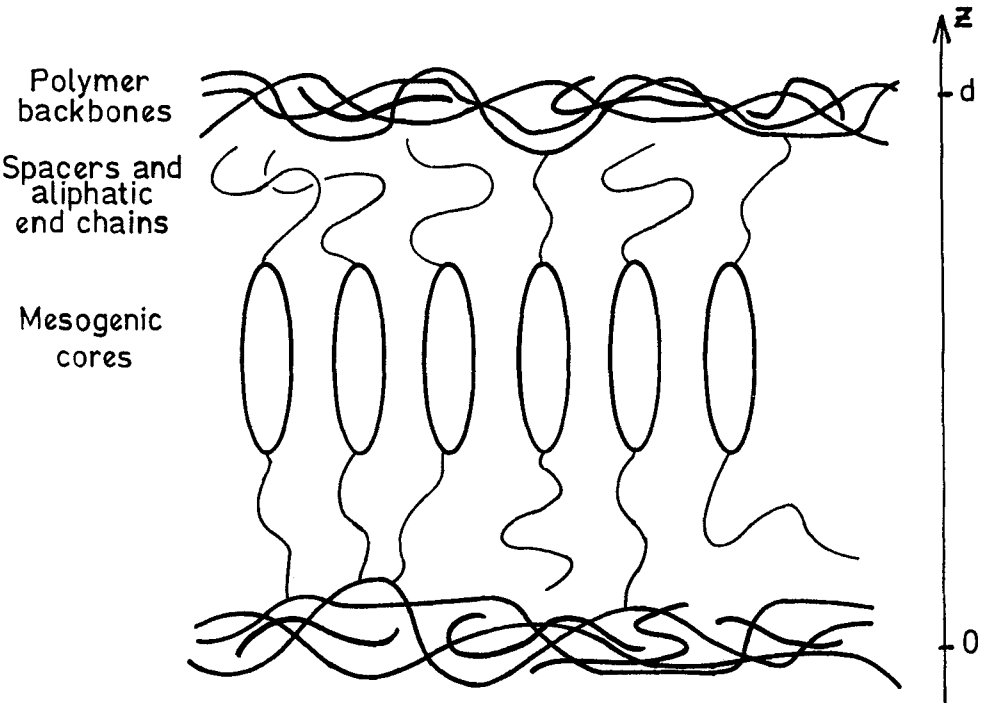

Figure 6. A sketch of the molecular organization of the $P_{3,4}$, $P_{4,4}$, $P_{3,8}$ and $P_{5,8}$ polysiloxanes in the S_A phase.

reflection making them unobservable. Indeed the compression constants B of S_{A_d} phases are known to be smaller than those of S_{A_1} phases [87]; this may hold true for polymeric phases too. In other words, S_{A_d} phases being more compressible than the S_{A_1} phases, the backbones are less confined and their electron density is spread out which explains why only one order of reflection can easily be detected for polymers $P_{4,1}$ and $P_{5,1}$. A systematic study of the absolute intensities of the reflections from the layers remains to be made in order to compare mesomorphic polymers and usual mesogens and to try to relate these intensities with the values of the elastic constants B when they are available.

A second example shows an unexpected effect occurring in a series of cyano-substituted mesomorphic side chain polyacrylates:

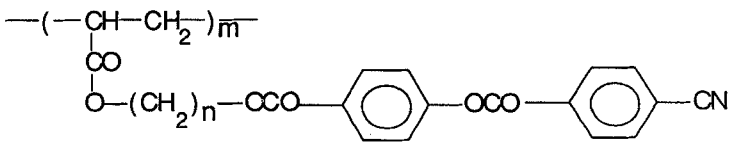

labelled P_n and synthesized by Strzelecki [8]. The presence of the cyano group at the end of the mesogenic core induces a partially bilayer organization ($l<d<2l$) in the smectic phase (S_{A_d} phase) [85]. Most members of this homologous series present the peculiarity that the third order of reflection from the smectic layers is abnormally strong if not the strongest. For a member, P_5, of this series the third order is even, by far,

Table 2. Amplitudes normalized to the third, of the different orders of reflection on the smectic layers for polymers P_5, P_8 and P_{12}.

	P_5	P_8	P_{12}
a_1	0	0·53	0·85
a_2	0·33	0·21	0·56
a_3	1	1	1

the strongest one (see table 2). This means that the electron density profile $\rho(z)$ is mainly described by the third order harmonic of period $d/3$ (figure 7). This experimental fact needs to be explained in terms of the molecular organization (figure 8). The parts (1) and (2) of $\rho(z)$ may be easily understood: part (1) corresponds to the region of overlap of mesogenic cores and therefore must have a large electron density. Since the packing of the mesogenic cores in this region determines their density within the smectic layer, the adjacent region (2) must have a density two times smaller. (It should be recalled here that we are only considering the difference between the density $\rho(z)$ and the mean density ρ_0.) It remains to understand the last two parts (3) and (4) of $\rho(z)$. Since both the backbones and the spacers in that case, are made of methylene groups, we can picture these regions as a modulated aliphatic medium expanded in the region of the backbones and compressed in the region of the spacers. Schematically, the backbones tend to expand in order to increase their entropy and therefore squeeze the spacers. Such an effect could best be detected for polymer P_5 since the lengths of the different parts (1)–(4) are all roughly equal to $d/6$ and then the third order sinusoidal function can develop smoothly in the unit cell.

The last example illustrates a comparison between the results obtained by small angle neutron scattering [62] and by X-ray diffraction. The polymers studied are several polyacrylates and polymethacrylates which have the formula

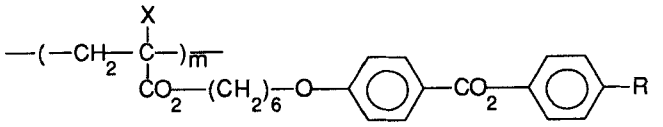

where $X = H$, CH_3 and $R = OCH_3$, OC_4H_9 and are labelled PAOCH3, PMAOCH3, $PAOC_4H_9$ and $PMAOC_4H_9$ according to X and R. Three of these polymers exhibit S_{A_1} phases and the amplitudes of the different orders of reflection (see figure 9) from the smectic layers have been measured (see table 3) [84]. From these measurements, the different electron density profiles $\rho(z)$ can be obtained (see figure 10) and discussed in relation to the different anisotropy ratios of the gyration radii ($\lambda = R_\perp/R_\parallel$) measured by small angle neutron scattering:

For $PMAOCH_3$ (see figures 9(*a*), 10(*a*) and 11(*a*)), only one order of reflection could be observed; $\rho(z)$ is described by a single sinusoidal function according to de Gennes' model. Thus the backbones hardly feel the smectic field and indeed the anisotropy ratio of gyration radii is rather small ($\lambda \approx 2$).

For $PAOCH_3$ (see figures 9(*b*), 10(*b*) and 11(*b*)), two orders of reflection can be measured and $\rho(z)$ shows a secondary maximum due to the backbones. The anisotropy ratio λ rises to about 4 showing that the backbones are better confined.

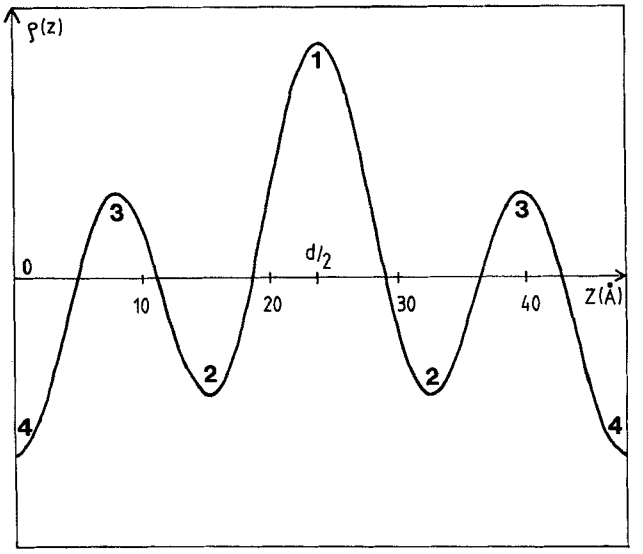

Figure 7. The electron density profile $\rho(z)$ of the cyanosubstituted P_8 polyacrylate in the S_A phase. The numbers 1, 2, 3 and 4 refer to the different regions defined in the text and in figure 8.

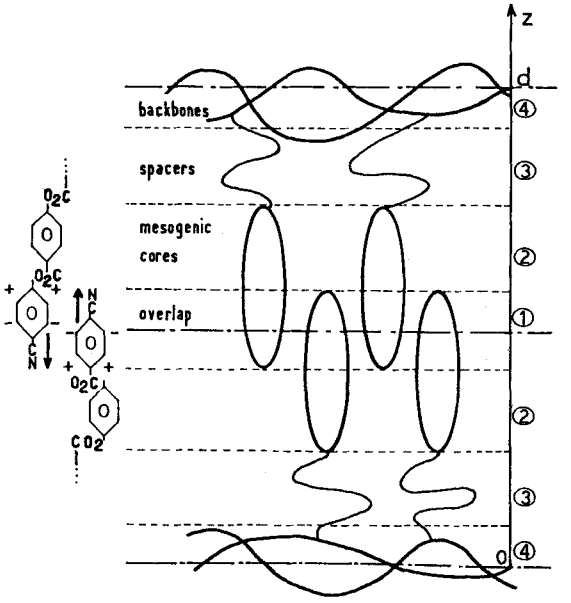

Figure 8. A sketch of the molecular organization in the S_A phase of the cyanosubstituted P_n polyacrylates. The numbers 1, 2, 3 and 4 correspond to the different parts of the electron density profile of figure 7.

Table 3. Amplitudes normalized to the first, of the different orders of reflection on the smectic layers for polymers $PMAOCH_3$, $PAOCH_3$ and $PMAOC_4H_9$.

	$PMAOCH_3$	$PAOCH_3$	$PMAOC_4H_9$
a_1	1	1	1
a_2	0	0·8	0·5
a_3	0	0	0·5

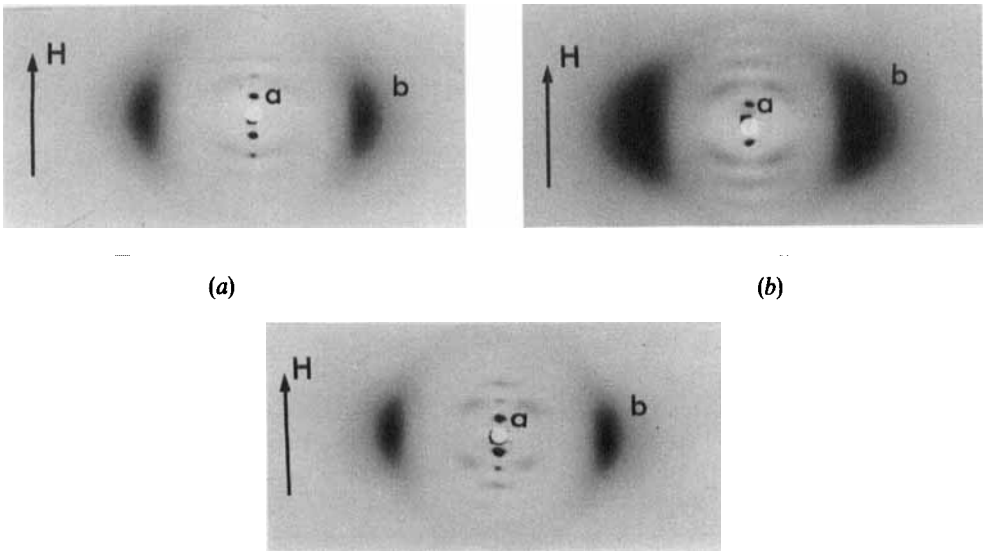

(*a*) (*b*)

(*c*)

Figure 9. X-ray diffraction patterns of two polymethacrylates and a polyacrylate in the S_A phase. a, Bragg reflections; b, wide angle diffuse ring; H is the magnetic field direction. The diffuse scattering is discussed in section 3. (*a*) $PMAOCH_3$ (over exposed because the Bragg reflections are very weak); (*b*) $PAOCH_3$; (*c*) $PMAOCH_4H_9$.

Finally $PMAOC_4H_9$ (see figures 9(*c*), 10(*c*) and 11(*c*)) displays three orders of reflection and its density profile is somewhat similar to that of $PAOCH_3$, the backbones are rather well-confined and indeed the anisotropy ratio λ is also roughly equal to 4. Moreover, in this case, $\rho(z)$ exhibits details in the region of the mesogenic cores; it seems that grafting aliphatic chains on each end of the mesogenic cores helps their packing in layers, probably reducing the longitudinal Debye–Waller factor so that $\rho(z)$ is less smoothed by longitudinal positional fluctuations. This last homologous series shows that the behaviour of the backbones may be apprehended in a similar way by X-ray diffraction and small angle neutron scattering.

2.2.3. *Comparison of the smectic period d with the side chain length l*

Usually, in the S_A phase of conventional (non-polar) mesogens, the smectic period d is roughly equal to the molecular length l. This eventually will not be the case if the mesogen has a strong electric dipole such as a CN group at one of its ends. This dipole

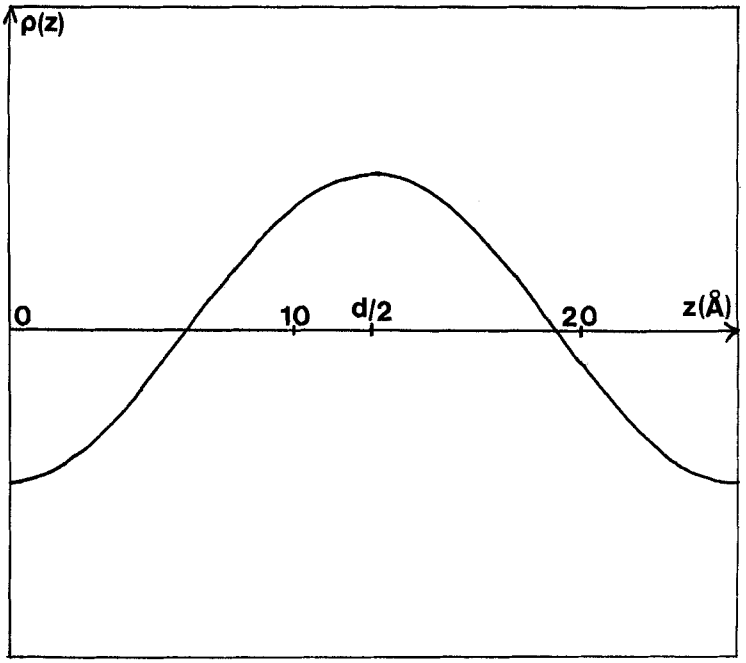

(*a*)

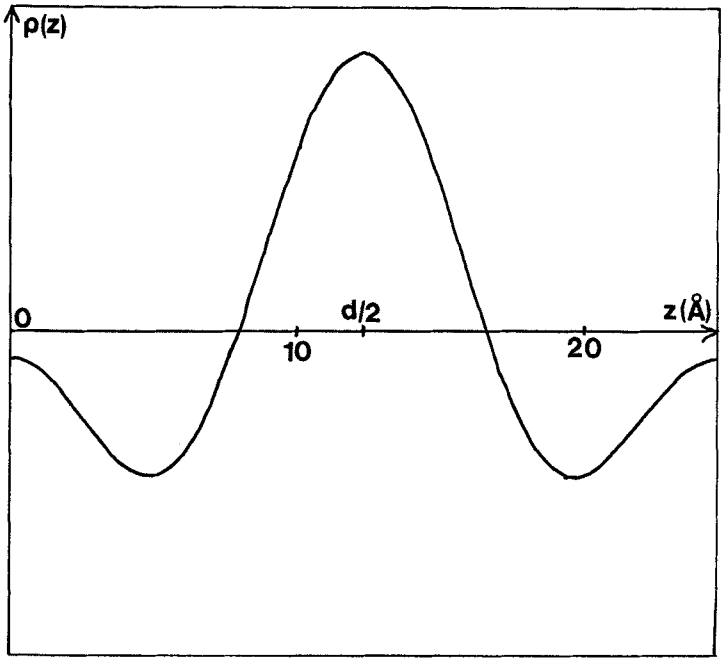

(*b*)

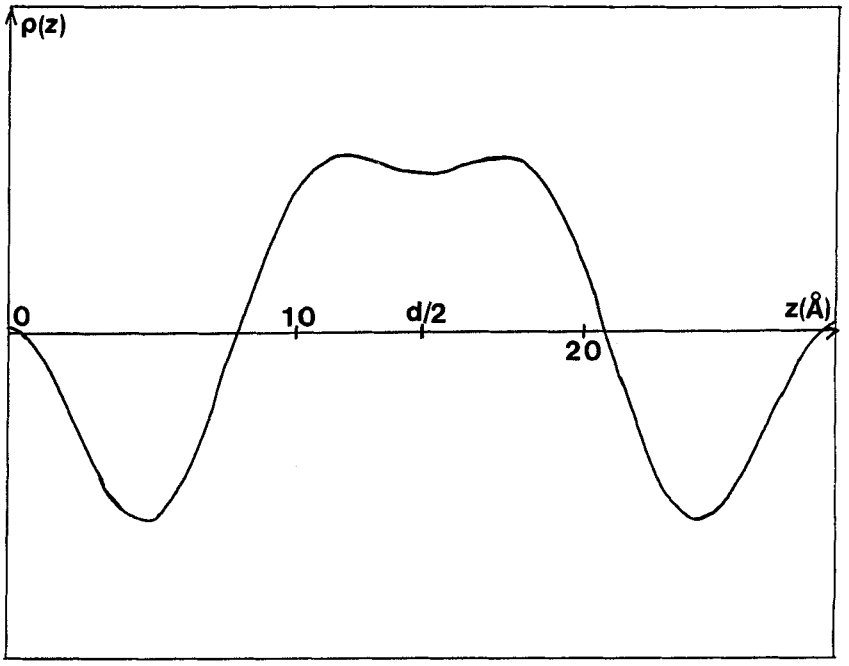

(*c*)

Figure 10. The electron density profiles $\rho(z)$ for the polymers $PMAOCH_3$, $PAOCH_3$ and $PMAOC_4H_9$ in the S_A phase. (*a*) $PMAOCH_3$, the profile is described by a single sinusoidal function; (*b*) $PAOCH_3$, the confinement of the backbones is responsible for the appearance of the secondary maximum at $z=0$; (*c*) $PMAOC_4H_9$, the backbones are rather well confined; moreover, details of the mesogenic core packing may be seen.

will induce the formation of antiparallel pairs of partially overlapping molecules. The smectic period d may then lie between once and twice the molecular length l, $l<d<2l$ (see figure 12(*a*)) and the smectic A phase is called S_{A_d}. (Many other smectic A modifications may also appear [85].) Mesomorphic side chain polymers do not need dipolar substituents to form S_{A_d} phases. For instance, the $P_{n,m}$ polysiloxanes (see § 2.2.2) form S_{A_1} ($d \approx l$) or S_{A_d} phases according to the relative values of n and m. A necessary condition to obtain a S_{A_d} phase is the possibility to define an up or down direction for the long axis of the mesogenic core. For a polar conventional mesogen, this condition is simply fulfilled by the presence of the dipole whereas for mesomorphic side chain polymer, this condition is fulfilled by the fact that the mesogenic core is attached to the backbone by only one of its ends (see figure 12(*b*)). A second condition is that the mesogenic cores should have a tendency to pack in a partially overlapping antiparallel way. This clearly arises from the dipolar interactions of polar conventional mesogens but the origin of such a tendency in polymeric systems has not yet been fully elucidated. It seems to be related to the existence of the backbone and might be due to a difference in packing at the (backbone and spacer) level and aliphatic tail level. Another explanation based on dipolar induced dipolar forces has also been suggested [88]. An interesting analogy can also be seen with a microscopic theory of polar conventional liquid crystals [89]: let us suppose that the in-plane short range environment of any

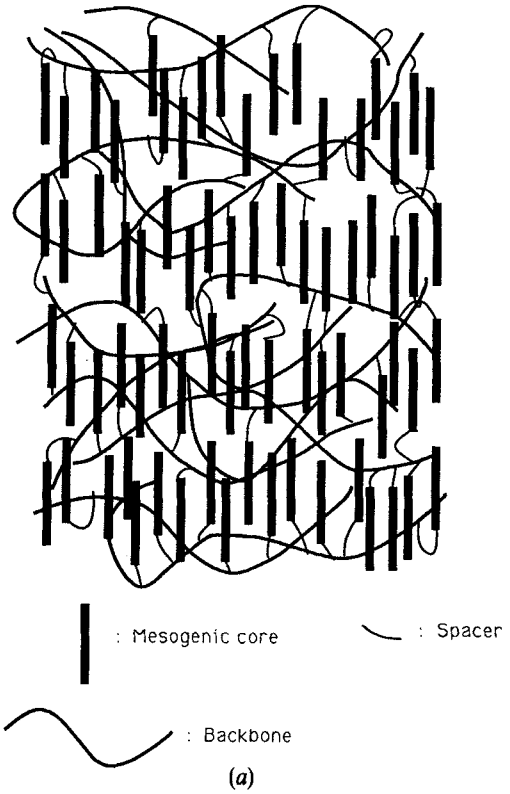

(*a*)

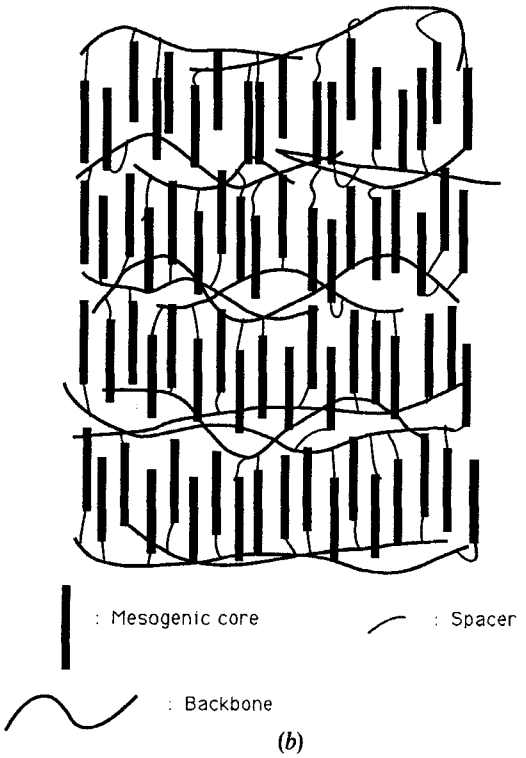

(*b*)

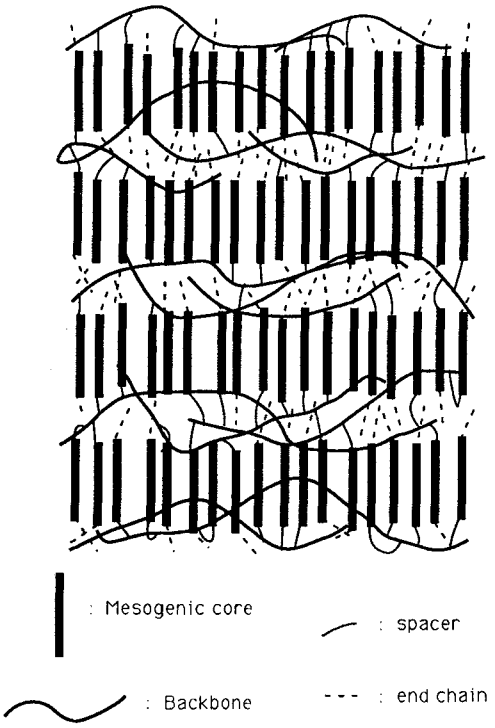

(*c*)

Figure 11. The molecular organization of the polymers $PMAOCH_3$, $PAOCH_3$ and $PMAOC_4H_9$ in the S_A phase. (*a*) $PMAOCH_3$, the smectic order is rather weak and does not affect the backbones very much; (*b*) $PAOCH_3$, the smectic order is stronger and the backbones are rather well confined between the sublayers of the mesogenic cores; (*c*) $PMAOC_4H_9$, the smectic order is quite strong due to the segregation of the smectic layer into three kinds of different sublayers: mesogenic cores, backbones, spacers and end chains.

given side chain in the S_A phase is hexagonal. The intrinsic frustration of an up-down ordering on this lattice may be relieved by considering that the backbone does not have this hexagonal symmetry so that for any triangle made of side chains, one of its sides is shorter than the other two. The backbone trajectories could be described as the successions of these shorter sides. The role of the backbones would then be to strengthen the up-down interactions by steric means. Anyway, two contradictory experimental observations show that this problem is complicated: in the series of $P_{n,m}$ polysiloxanes [19], S_{A_d} phases are obtained for $n>m$ and S_{A_1} for $n<m$ whereas in another series [32] the opposite situation seems to prevail. Therefore, no general behaviour can be clearly demonstrated.

This problem may be reduced to a simpler version by only considering the conditions of occurrence of the S_{A_2} phase ($d \approx 2l$). This question may be easier to answer since it only deals with the competition between the two extreme cases illustrated in figures 13 (*a*) and (*b*). Figure 13 (*a*) corresponds to the simple S_{A_1} phase in which the backbone density is modulated with a period $d \approx l$. Figure 13 (*b*) corresponds to the S_{A_2} phase (a kind of antiferroelectric phase) in which the backbone density is modulated with a period $d \approx 2l$. There is no mesogenic core overlap in this phase. Only very few

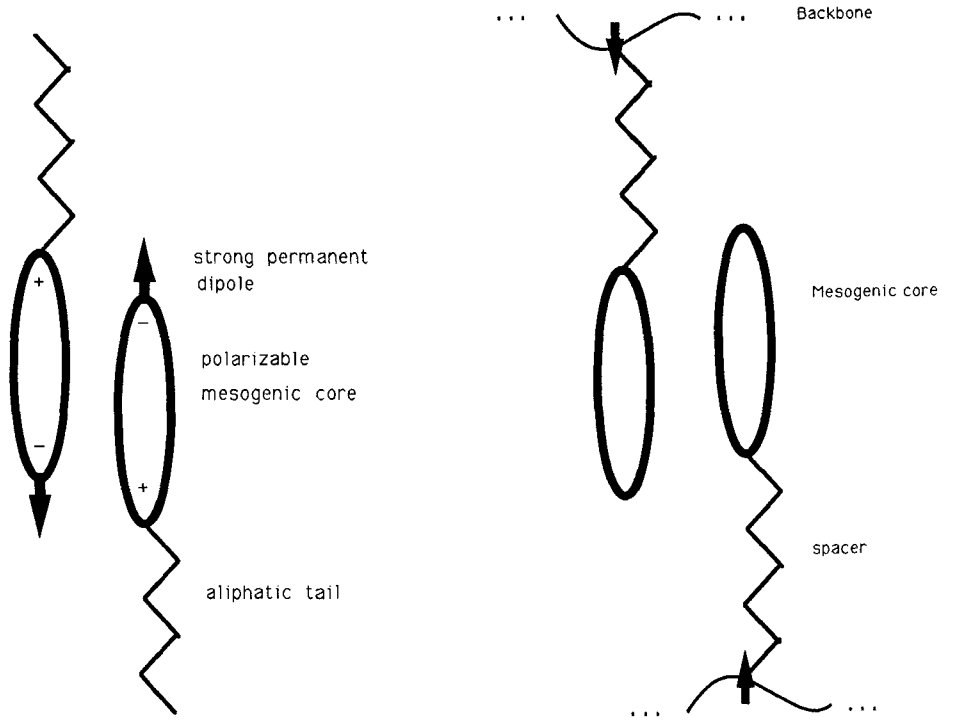

Figure 12. Association of two mesogenic cores in an antiparallel partially overlapping fashion. (*a*) Due to dipole interactions for polar low molar mass mesogens; (*b*) due to the existence of the backbone for mesomorphic comb like polymers.

comb-like polymers were reported to exhibit a true S_{A_2} phase ($d \approx 2l$). They do not bear any strong dipoles but all possess very short spacers though this is not a sufficient condition in itself. For instance, figure 14 shows the X-ray diffraction pattern of an aligned sample of a polyacrylate

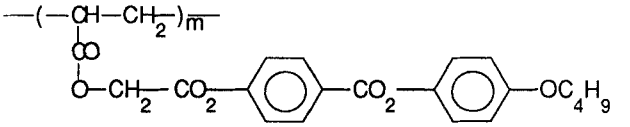

labelled PA(1)OC_4H_9, in its S_{A_2} phase ($d = 40$ Å, $l = 21$ Å).

2.2.4. *Influence of the mesogenic cores grafting rate upon the molecular organization*

Only very few structural studies have been made in this domain and they can be summarized as follows: partial grafting of the mesogenic cores (i.e. the dilution of the cores on the backbone) does not destabilize the smectic phases until rather low grafting rates are reached. (It was even possible to keep the S_A phase with grafting rates as low as 10 per cent [30,90]. However, the polymers studied were polysiloxanes and the backbones might show a segregation effect which could stabilize the lamellar phase.) The smectic A organization is not affected except that the smectic period increases when the grafting rate decreases. This was explained by assuming that the backbones fold themselves and increase their width along the director.

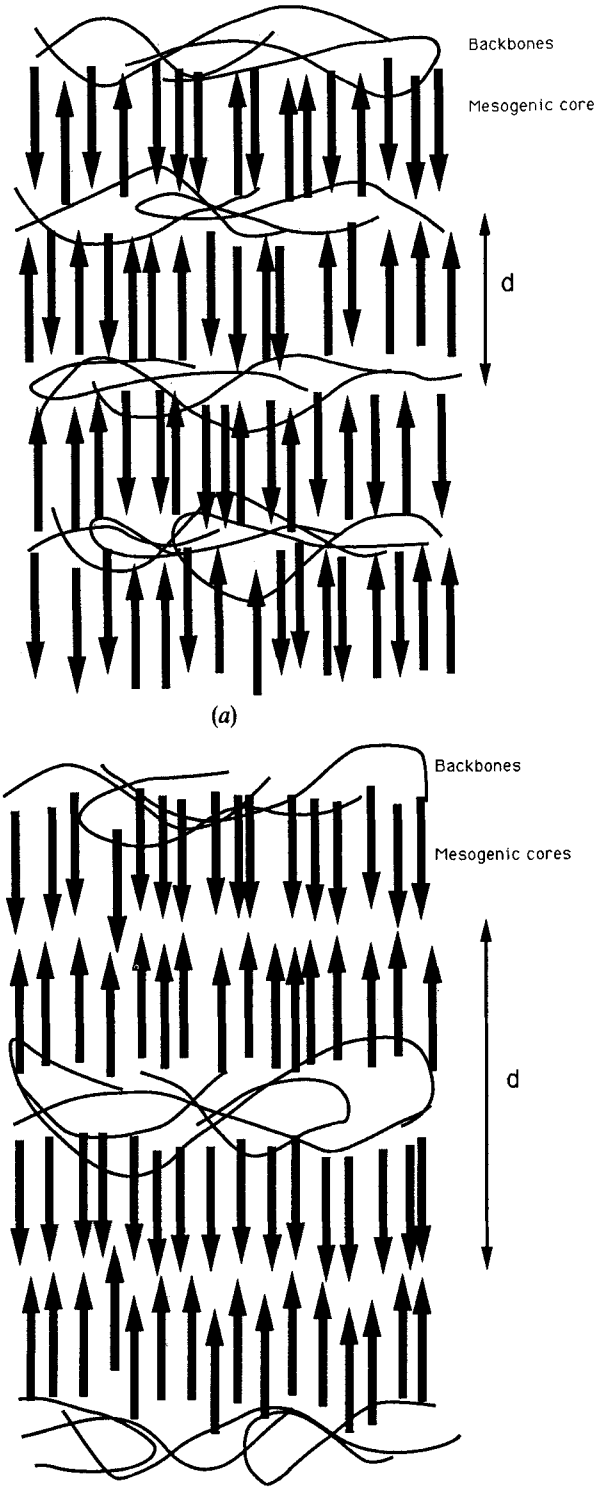

Figure 13. (*a*) A schematic representation of the S_{A_1} phase in which each layer is made of randomly oriented side chains ($d=l$). (*b*) A schematic representation of the S_{A_2} phase in which each layer is made of side chains oriented in the same direction. Its smectic period involves two such layers ($d=2l$) and the backbone distribution along the director is modulated with the period d.

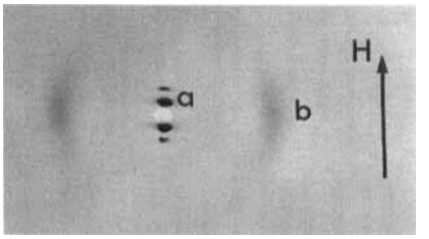

Figure 14. X-ray diffraction pattern of the polyacrylate PA(1)OC_4H_9 in its S_{A_2} phase. a, Bragg reflections; b, wide angle diffuse ring; H is the magnetic field direction.

Conversely, doubling the grafting rate was made possible by synthesizing polymers which bear two mesogenic cores on the same backbone repeat unit [37, 91]. This case is illustrated by a polyitaconate series [91]

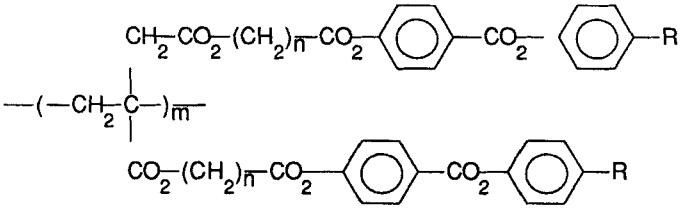

Let us consider polymer $n=5$ and $R=OC_4H_9$ called $PI_{5,4}$, of this series; it forms a N phase and a S_{A_d} phase, whereas the corresponding polyacrylate $PA_{5,4}$ which has only one mesogenic core on each repeat unit forms a N phase, a metastable S_A phase and a crystalline lamellar phase [5]. (This difference may eventually only be due to a difference in the degree of polymerization.) The X-ray diffraction patterns of both polymers in the nematic phase are similar. Moreover the smectic period of the polyitaconate is equal to the lamellar spacing of the polyacrylate.

In addition, a polycomaleate series was also synthesized [92] in order to study the influence of the grafting sequence upon the organization. The corresponding polycomaleate called $PM_{5,4}$

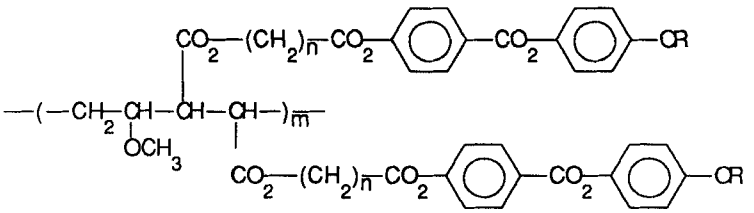

forms a N phase and a metastable S_{A_d} phase. The X-ray diffraction patterns of $PM_{5,4}$ in both phases are quite similar to those of $PI_{5,4}$ and $PA_{5,4}$.

All of these results show that the molecular organization is not very sensitive to the grafting rate of the mesogenic cores and their sequence.

2.3. *The smectic C phase*

The case of the S_C phase is more complicated than that of the S_A since the S_C phase is biaxial [13]. By the usual means of alignment (magnetic field or fibre drawing), only

samples of uniaxial symmetry can be produced which induces a loss of information. Figure 15 shows an example of an X-ray diffraction pattern from a mesomorphic comb-like polysiloxane labelled $PSOC_4H_9$ in the S_C phase [84, 93] cooled in a magnetic field; its formula is

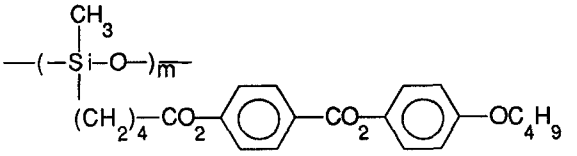

Three orders of reflection from the smectic layers can be seen in this pattern. This means that the electron density profile can also be derived in the S_C phase and can be treated in the same way as in the S_A phase. In addition, the increase of the smectic correlation length versus temperature and its saturation were also observed within the S_C phase [52] and also interpreted in terms of the influence of the backbone. Indeed, most of what has been said about the mean structure of the S_A phase can clearly be extrapolated to the S_C by simply introducing a tilt angle between the director and the normal to the layers. More specifically, Keller *et al.* [57] have also found an unexpected effect: in the polymeric S_C phase, the tilt angle decreases with decreasing temperature which is just the opposite behaviour to what is usually observed for low molar mass mesogens. This effect was interpreted as arising from a stiffening of the backbones.

The S_C phase is particularly interesting in view of technological applications because its chiral version, the S_C^* phase thanks to its symmetry, can present a spontaneous polarization [94]. Therefore, a large number of X-ray characterization studies have focused upon the polymeric S_C and S_C^* phases [6, 11, 13, 22, 32–34]. However, because of its chirality, the S_C^* phase forms a helical superstructure which makes the X-ray diffraction patterns more difficult to understand. It is often necessary, therefore, to unwind the helix by applying a strong enough external field or by drawing fibres. X-ray diffraction patterns typical of the S_C phase are thus obtained and allow an unambiguous phase assignment.

2.4. *The smectic B phase*

We quickly recall the structure of the conventional S_B phase [95]. The S_B phase differs from the S_A by the fact that the molecules have some type of long range ordering within each layer. In this domain we should consider two types of ordering: the positional order (of hexagonal symmetry) inside the layer and what is called the bond

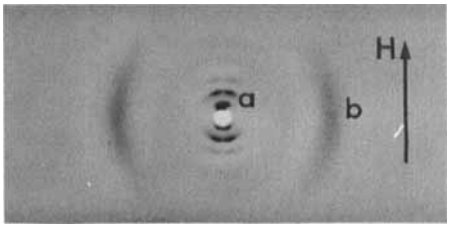

Figure 15. X-ray diffraction pattern of the polysiloxane $PSOC_4H_9$ in its S_C phase. a, Two rows of Bragg spots (which represent the intersection of reflection rings with the Ewald sphere) make a finite angle with the director aligned by the magnetic field *H;* b, wide angle diffuse ring.

orientational order which describes the orientation of the vectors joining two neighbouring molecules in the same layer. According to the strength of the interlayer correlations, these two different types of ordering may be short range, quasi long range or long range. Our aim here is not to discuss this question (see [95] and references therein) but we shall summarize the situation by stating that two kinds of S_B phase exist: the crystal B and the stacked hexatic B phases. If the interlayer correlations extend over a long range, then the molecules are three dimensionally correlated and the phase is called a crystal B and should be considered a kind of orientationally disordered crystal rather than a true liquid crystal. Another phase made of stacks of two dimensional hexagonal lattices is callled a stacked hexatic B phase. In this phase, the positional order within a layer is only short range whereas the bond orientational order remains long range and is three dimensionally correlated. At this point, the question arises as to how to determine which class the polymeric S_B phase belongs to.

From another point of view, we can also try to compare the polymeric S_B phase with crystals of polymers. These crystals often have a large amount of disorder called of the second kind [96]. This type of disorder is different from the usual type (called the first type, such as thermal fluctuations) because it does not preserve an average lattice at long range. Therefore, the positional long range order is destroyed and consequently the Bragg reflections are broadened proportionally to their indices. In the field of polymers, such a description is called the paracrystal model of Hosemann [97]. Let us now consider the polymeric S_B phase [10, 23, 47, 49, 50, 53, 54]. First, the electron density profile along the normal to the layers can be obtained in exactly the same way as that used for the S_A phase. Figure 16 shows the electron density profile of polymer $P_{3,8}$ in the S_B phase. This profile looks very much like that of the S_A phase except that the backbones are somewhat better confined and that details appear in the region of the

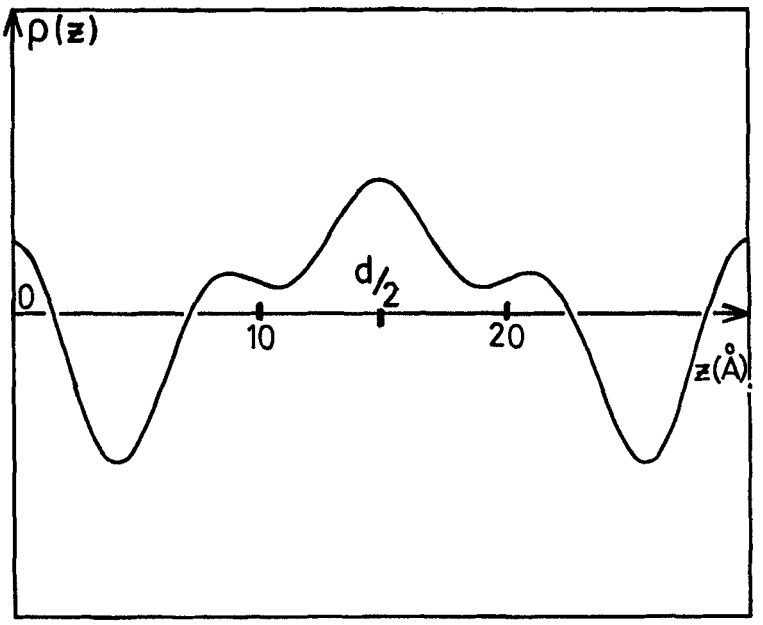

Figure 16. The electron density profile $\rho(z)$ of polysiloxane $P_{3,8}$ in the S_B phase. The region of mesogenic cores exhibits details because the longitudinal Debye–Waller factor is smaller in the S_B phase than in the S_A.

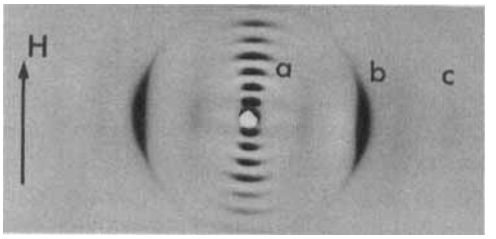

Figure 17. X-ray diffraction pattern of the polysiloxane $P_{3,8}$ in the S_B phase. a, (00*l*) reflections on the smectic layers; b, (100), and c (110) hexagonal lattice reflections within each smectic layer; *H* is the magnetic field direction. The diffuse scattering is discussed in § 3.

mesogenic cores possibly because of a lower Debye–Waller factor. Thus the electron density profile does not reveal any specificity of the S_B phase. Moreover, it should be noted that the Bragg reflections from the layers are not resolution limited [49, 50, 54] so that the smectic ordering extends only over about 1000 Å. Furthermore, this ordering improves when the temperature increases; this behaviour is similar to those of the polymeric S_A and S_C phases and was explained in the same way. (The same conclusions were also drawn from a similar study of the polymeric S_F phase [52].) Therefore, the polymeric S_B phase differs considerably from the crystal B type in this respect.

Figure 17 shows the X-ray diffraction pattern of $P_{3,8}$ in the S_B phase. The most important fact is that no three dimensional reflection (i.e. the reflections with $h \neq 0, k \neq 0$ and $l \neq 0$) can be detected. This means that the polymeric S_B phase does not have any long range three dimensional positional correlations. Therefore, it is not of the crystal B type. A similar situation was also observed [14, 17, 18] in the case of a polymeric S_E phase. It seems that the presence of the backbone tends to decorrelate adjacent smectic layers and thus prevents the propagation of the crystalline order along the director. Along the equator, *hk*0 reflections can be detected which are characteristic of the hexagonal lattice of the mesogenic cores within the smectic layers. It should be noted that because of the orientation process (magnetic field), the sample has a fibre geometry, i.e. a uniaxial symmetry around the director. All attempts to produce monodomains of the polymeric S_B phase were unsuccessful. An important observation is that the widths of the *hk*0 reflections are not resolution limited [10]; these widths increase with increasing *hk* indices. Therefore, the in-plane positional order does not extend over a long range. On the one hand, this observation is consistent with a paracrystal picture and the amplitude of fluctuation of the hexagonal lattice vector could be estimated to be $\langle \Delta a^2 \rangle^{1/2} \approx 0{\cdot}7$ Å which is roughly 10 per cent of the distance between mesogenic cores. On the other hand, this observation is also consistent with the stacked hexatic B phase. (These two pictures are in no way contradictory since the paracrystal model only states the mean square value of the fluctuations whereas the hexatic model gives a complete microscopic description of the organization.) Indeed the width $\Delta(2\theta) = 0{\cdot}75°$ of the 10 reflections of the polymeric S_B phase is comparable to that of the stacked hexatic B phase of conventional mesogens. The hexatic model predicts a Lorentzian shape for the *hk*0 reflection profiles; however, this could not be checked properly because of the uniaxial symmetry of the sample which results in a two dimensional powder distribution. True monodomains of a polymeric S_B phase are therefore needed to check if the hexatic model is really valid here.

3. Short range order

In this part, we describe the different kinds of short range order which disturb the average structures presented in § 2. From the experimental point of view, let us just recall [96] that the average structure is obtained from the exploitation of the resolution limited reflections whereas short range order gives rise to the so-called diffuse scattering which is an X-ray intensity scattered in a large solid angle. Usually, the angular spreads of this diffuse scattering in each direction are inversely proportional to the correlation lengths of the short range order. Now, the symmetry of a mesophase is determined by the nature of the long range order that it displays. Nevertheless, this mesophase may also have various types of fluctuations of lower symmetry extending only over a short range. These fluctuations can be divided into two kinds.

They may be pretransitional effects, just above the phase transition. For instance, S_A or S_C fluctuations are readily observed in the polymeric nematic phase [56, 58]. It may also happen that, in a given mesophase, pretransitional fluctuations are observable but that on decreasing the temperature, the corresponding phase transition

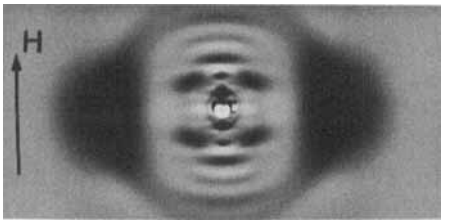

(*a*)

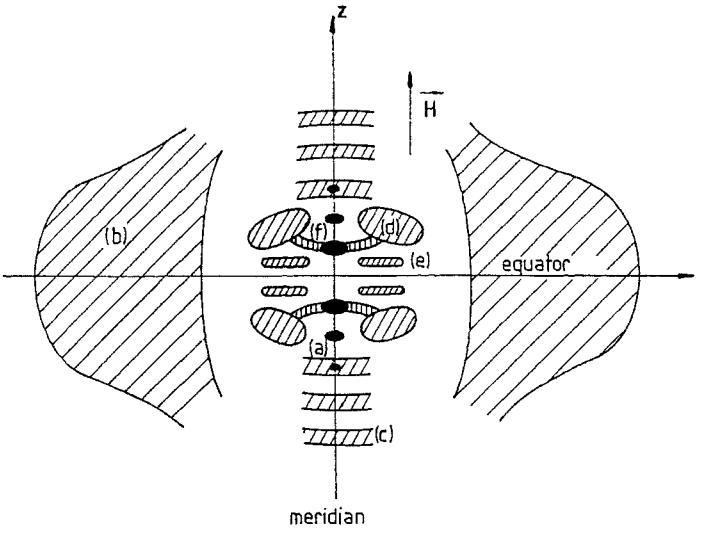

(*b*)

Figure 18. (*a*) Over exposed X-ray diffraction pattern of the polymer PMA(H,D)OC_4H_9 (H, protonated backbone; D, deuteriated backbone) in the S_A phase. The pattern actually represented is that of PMA(D)OC_4Hg. *H* is the magnetic field direction. (*b*) A schematic representation of (*a*): a, Bragg reflections on the smectic layers; b, wide angle diffuse ring; c, diffuse streaks; d, large diffuse spots; e, small diffuse spots in the case of PMA(H)OC_4H_9 and small diffuse streaks in the case of PMA(D)OC_4H_9; f, small tilted diffuse streaks called 'moustaches'.

cannot be observed because of the occurrence of the glass transition [98]. These pretransitional phenomena are sometimes called diffraction by cybotactic groups. (This vocabulary is rather misleading since it suggests that the phase is made up of small domains with well-defined borders and within which the lower symmetry order prevails.) From the position in reciprocal space of the resulting diffuse scattering, an apparent side chain (and backbone segment) length and eventually an apparent tilt angle may be obtained. From the profile of the diffuse scattering, the correlation lengths of these fluctuations may also be obtained [56, 58]. We shall not consider these pretransitional phenomena any further in this article.

For polymeric mesophases, the appearance of fluctuations is more frequently due to the short range correlations induced by the backbone among neighbouring mesogenic cores. Indeed a comparison between over exposed X-ray diffraction patterns of, for instance, the S_A phase of a conventional mesogen and a mesomorphic comb-like polymer (see figures 18 (*a*) and (*b*)) shows that in the latter case, a large part of the scattered intensity is found in reciprocal space, outside the Bragg reflections (a) and the wide angle diffuse crescents (b). This additional diffuse scattering (c), (d), (e) and (f) is located in regions of reciprocal space which indeed correspond to correlations between different side chains. It seems that this particular diffuse scattering is much weaker than the Bragg reflections. However, it should be remembered that the Bragg reflections are resolution limited (using a conventional low resolution X-ray apparatus) whereas the diffuse scattering lies in large regions of reciprocal space and only the respective integrated intensities should be compared. In a first approach, these diffuse intensities (c), (d), (e), (f) may be treated separately; this implies that the corresponding short range orders are only weakly correlated if they are correlated at all. Most of the diffuse elements ((c), (d) and (e) in figure 18 (*b*) for instance) arise from the kind of short range order mentioned previously, but some other diffuse elements like (f) may only be explained in terms of localized defects such as edge dislocations. These localized defects will be discussed in §4. In the following, we shall describe the short range orders displayed by the polymeric S_A and S_B phases, though some of these ideas also apply to other polymeric smectic phases or even to the polymeric nematic phase if it has strong enough smectic fluctuations.

3.1. *Uncorrelated longitudinal disorder*

Many X-ray diffraction patterns of mesomorphic comb-like polymers have diffuse streaks perpendicular to the director. Two kinds of such diffuse streaks may appear and should not be confused.

The first kind is that of one or a few wide and curved diffuse streaks. Usually, they do not exhibit any periodicity along the director, or if they do, their period is clearly smaller than the side chain length. These streaks result from intramolecular interferences and do not give any information about the molecular organization in the mesophase but rather about the internal chemical structure or conformation of the molecule. Such diffuse streaks are more readily observed if the polymer repeat unit (backbone or side chain) has a heavy atom such as a chlorine or even a silicon atom [38] (see figure 4 (*b*)). This kind of diffuse streak may also be observed in the X-ray diffraction patterns of conventional mesogens.

The second kind consists in a set of straight, equidistant diffuse streaks with a well-defined periodicity along the director (diffuse element (c) in figure 18 (*b*)). This periodicity is usually equal to the side chain length; it can be larger if the side chains

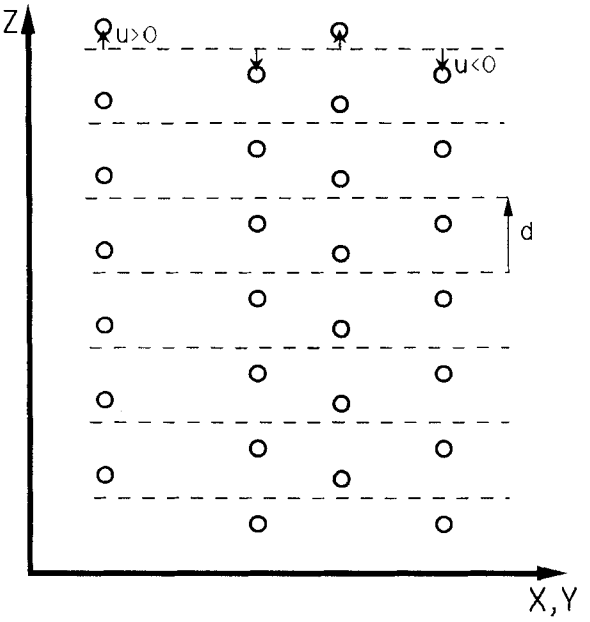

Figure 19. Uncorrelated longitudinal disorder. The small circles may represent either atoms in the case of $KNbO_3$ or the centres of gravity of side chains in the case of mesomorphic comb-like polymers. Four vertical uncorrelated rows have been represented. d is the lattice spacing, in our case the smectic period. **u** is the displacement vector which is the same for all the rows for $KNbO_3$ but which may well vary for different rows for mesomorphic comb-like polymers.

tend to form overlapping antiparallel pairs. These diffuse streaks correspond to the intersection with the Ewald sphere of a series of equidistant diffuse planes. These diffuse planes represent the Fourier transform of a linear modulated object oriented along the director [96]. This type of diffuse streak may sometimes be observed in the X-ray diffraction patterns of both polymeric [84, 99] and conventional [100] nematic phases. In this case, it means that the molecules tend to align themselves in rows over a short range. The correlation length of this ordering process may be estimated from the width of the diffuse streaks along the director.

The same type of diffuse streak may often be found in the X-ray diffraction patterns of the polymeric smectic phases. Because of the existence of the one dimensional lattice, they must be interpreted in a slightly different way: the rows are made of mesogenic cores which are longitudinally displaced out of their mean positions in the layers. Such a description assuming an uncorrelated linear disorder was first given to account for the existence of diffuse planes in the X-ray patterns of $KNbO_3$ [101] and related compounds and was then applied to conventional crystal B phases [102]. We shall only mention here the results of this description [101]: let us call **d** the smectic periodicity vector, f the form factor of the side chain, **s** the scattering vector ($s=2\sin\theta/\lambda$ where 2θ is the scattering angle), **u** the displacement of the side chain out of its mean position in the layer and N the number of side chains in the rows (see figure 19). Furthermore, let the rows be completely uncorrelated. The scattered intensity is then given by

$$I(\mathbf{s})=\frac{f^2\sin^2(N\pi\mathbf{s}\cdot\mathbf{d})}{\sin^2(\pi\mathbf{s}\cdot\mathbf{d})}\sin^2(2\pi\mathbf{s}\cdot\mathbf{u}).$$

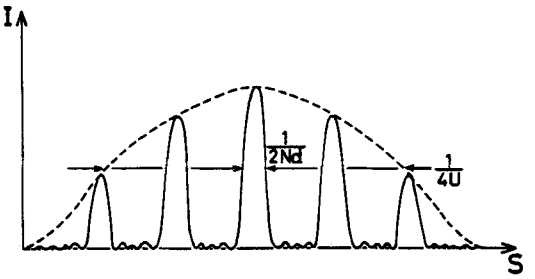

Figure 20. X-ray scattered intensity in a direction parallel to the director. Each peak represents a diffuse plane. Their intensities are modulated by a factor $\sin^2(2\pi \mathbf{s}\cdot\mathbf{u})$ related to the displacement vector **u**.

The X-ray scattering is essentially localized in equidistant parallel planes of periodicity $1/d$ and perpendicular to the director (see figure 20). Their width along the director is $1/Nd$, thus inversely proportional to the length of the row. No meridional diffuse plane can be found since $\mathbf{s}\cdot\mathbf{u}=0$. The diffuse planes intensities are proportional to $\sin^2(2\pi \mathbf{s}\cdot\mathbf{u})$ and so the amplitude of the longitudinal displacement can also be estimated. Finally, in a given diffuse plane, the intensity is only described by the transverse form factor of the row which is that of the side chains in most cases. For instance, $PMAOC_4H_9$ [4] and other related polymers give diffuse streaks which can be interpreted in this way, leading to an average longitudinal displacement u of about 4 Å and a longitudinal correlation length of about 150 Å. Several $P_{n,m}$ polysiloxanes also have this kind of diffuse streaks in both the S_A and S_B phases [10].

The case of the S_{A_d} phases can be more complicated if the columnar periodicity is equal to the molecular length l whereas the smectic periodicity is not ($l<d<2l$) [4]. Then, we must consider that inside the S_{A_d} matrix, there exist linear defects made of side chain rows of period l. This implies that these rows are no longer related to the smectic periodicity. In particular, their form factor must be different from that of the layers so that the intensity distribution of the related diffuse planes does not follow that of the Bragg reflections. It should be noted that these defects do not give rise to any appreciable small angle X-ray scattering, probably because their global electronic density is still too close to that of the S_{A_d} matrix.

3.2. *Layer undulations*

Large diffuse spots such as (d) in figure 18 (*b*) are frequently observed in the X-ray diffraction patterns of polymeric mesophases [4, 5]. They cannot be explained in terms of pretransitional phenomena because this would not lead to acceptable values of the side chain length and sometimes also because too many of them can be detected. These diffuse spots are usually located in the same reciprocal planes perpendicular to the director as the Bragg reflections but this is not always the case. Actually, because of the uniaxial symmetry of the S_A phase these spots represent the intersection of diffuse tori with the Ewald sphere. Generally such a diffuse torus cannot be found in the equatorial plane.

First, we consider the case of diffuse spots located in the same (00l) reciprocal planes perpendicular to the director as the 00l Bragg reflections. This situation is illustrated by Figure 18 (*a*) which if inspected carefully shows that a diffuse torus of the same diameter as (d) but much broader, also exists in the (003) reciprocal plane. Since this torus is

much broader, then its signal-to-noise ratio is much smaller and it can merely be detected in figure 18 (*a*). The simplest way to explain the origin of these diffuse tori is to consider a transverse modulation of the smectic layers, of wavevector **a** and polarized along the director. The modulus of **a** ($a \approx 18$ Å) is given by the inverse of the tori radius. Since the modulations of adjacent layers are in phase, we can consider a two dimensional local ordering based on the wavevector **a** and the smectic period **d**. The diffuse torus (d) may then be labelled 102. The fact that no such torus can be found in the equatorial plane shows that the modulation of the layers is purely displacive; thus the overall density remains uniform. Moreover, in a given (00*l*) reciprocal plane, no other *hkl* diffuse spot other than 10*l* can be detected. Therefore the modulation may be considered to be sinusoidal. (Actually, a different model [5] for which the modulation is described by a square wave leads to similar results and though physically questionable, cannot be distinguished from the sinusoidal model on the basis of X-ray scattering evidence.) This undulation model is summarized schematically in figure 21 where a purely displacive, transverse sinusoidal modulation of the layers is depicted. Neither should these undulations be confused with the common thermal fluctuation modes of smectic layers [82] which usually occur in conventional S_A phases with wavelengths of a few 100 Å. At this point, we should remember that the 10*l* diffuse spots being quite broad, this two dimensional ordering is only correlated over a short range. Its correlation length is typically about 50 Å. Moreover, in the absence of any other *hkl* diffuse spots of higher indices than 10*l*, and because of the S_A phase uniaxial symmetry, no information can be obtained about the symmetry of this short range order inside the layers. Therefore, in the following, we shall only consider a local two dimensional ordering built upon **a** and **d**, bearing in mind that the smectic period **d** is well defined whereas the modulation wavevector **a** is submitted to large fluctuations.

The intensities and widths of the different 10*l* diffuse spots must now be explained too, all the more so since these intensities do not follow those of the Bragg reflections [4, 5]. First, the short range order affects these intensities (compared to the

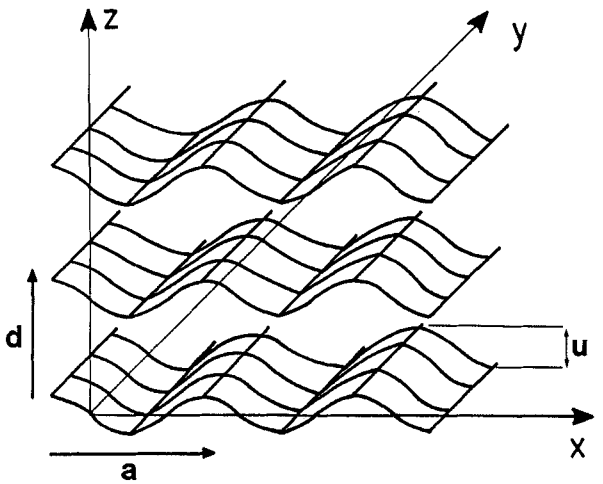

Figure 21. A local undulation model for the backbone sublayer. *d* is the smectic period, *u* is the undulation amplitude and *a* is the undulation period. The backbone performs a more or less two dimensional walk on the undulating surface. This model does not predict the kind of symmetry which prevails at short range within the smectic layers.

background) and widths. We can either use the model of second type disorder developed by Guiner [96] or the paracrystal model devised by Hosemann [97] since both methods are more or less equivalent and give similar results. The effect of second type disorder is to give a finite width to the Bragg reflections of the lattice it affects. The width of a diffuse *hkl* spot increases with increasing *hkl* indices. Moreover, the integrated intensity should remain constant and is only governed by the form factor. However, to be detected, a diffuse spot must have a maximum intensity appreciably larger than that of the background. This explains why the higher order 104 and 105 diffuse spots cannot be seen. Still using this formalism, the special shape of the 10*l* reflections can also be justified qualitatively. This shape is due to the fact that the fluctuations of vectors **a** and **d** are purely transverse [4, 5]. However, this formalism cannot explain why the 102/101 diffuse spots intensity ratio is completely different from that of the 002/001 Bragg reflections (actually, the 101 diffuse spot cannot even be detected in the pattern). To understand this fact, we must consider that the disorder is purely displacive and that the structure factor governing this modulation is different from that of the smectic layers, i.e. only part of the layer undulates. The electron density profile of the smectic layer may be represented here by step functions: the electronic density of the mesogenic cores may be taken as the origin since X-rays are only sensitive to the electronic contrast between the different moieties. Moreover, if we call p and q the respective widths of the region of the backbones and of the spacers, their electronic densities will be labelled n and $-np/p+q$ (see figure 22) so that the diffuse intensity starts from zero at the origin of reciprocal space as should be the case for a purely displacive disorder. According to this notation, the form factor of the undulating part of the layer will be

$$F(s_z)=\left[\frac{np\sin\pi s_z p}{\pi s_z p}-\frac{np\sin\pi s_z(p+q)}{\pi s_z(p+q)}\right],$$

where s_z is the z component along the director of the scattering vector **s**; n is not a relevant parameter since the relative intensities only should be considered here. Let us assume that the displacement follows the sinusoidal equation

$$z=\frac{u}{2}\cos\frac{2\pi x}{a},$$

where u is the displacement amplitude (see figure 21). Its Fourier transform will then describe its contribution to the intensity scattered along the $[h0s_z]$ reciprocal row as a term $J_h^2(\pi u s_z)$ where J_h is the Bessel function of order h. Finally, the diffuse scattering intensity $I_h(s_z)$ versus s_z along the reciprocal row $[h0s_z]$ will combine the two factors

$$I_h(s_z)=J_h^2(\pi u s_z)\left[\frac{np\sin\pi s_z p}{\pi s_z p}-\frac{np\sin\pi s_z(p+q)}{\pi s_z(p+q)}\right]^2$$

and we are only interested in the first $[10s_z]$ row. The fit parameters are p, q and u and the following values are obtained: $p\approx 6$ Å, $q\approx 4$ Å and $u\approx 10$ Å; they are in good agreement with estimates made with molecular (Dreiding) stereomodels and with the values derived in § 2 by inspecting the electron density profiles. In conclusion, the different intensities and widths of the diffuse spots may be explained by considering the effects of a second type disorder and that only part of the layer undulates. The same type of diffuse spots are also found in the X-ray diffraction patterns of the $P_{3,8}$, $P_{4,8}$ and $P_{5,8}$ polysiloxanes in the S_A phase. In that case, a large number of diffuse spots may be seen: 101, 102, 103 and 104 can easily be detected. Moreover, the 101/102 intensity ratio of

the diffuse spots is not very different from that of the 001/002 Bragg reflections. Indeed, the diffuse intensities may be accounted for by assuming, this time, that the whole layer undulates so that the diffuse intensities follow the smectic layers structure factor. No other *hkl* diffuse spot appears on the X-ray diffraction pattern which leaves unsolved the problem of the in-plane modulation symmetry.

We now comment upon the nature and possible origins of these undulations: their existence implies that there are small regions in which the backbone sublayer is bent. This sublayer presents a local array of mounds and wells. In these domains, the spacers should have a splay-like configuration with probably all the side chains pointing in the same direction (see figure 23). In the case of $PMAOC_4H_9$, considering circular mounds and wells of diameter ≈ 10 Å, their area will be roughly 100 Å^2 so that about five mesogenic cores are needed to build up one domain. The detailed conformation of a given backbone cannot be obtained from these X-ray scattering experiments. Fortunately, small angle neutron scattering experiments have been carried out on this compound and the gyration radii of the backbone have been measured [62]. The value obtained for the gyration radius in the layer plane $R_\perp \approx 100$ Å shows that a single backbone runs through a fairly large number of these mounds and wells. In a previous paper [4], we had suggested two possible explanations for the origin of such undulations. The first was that the natural tendency of the backbone to be disordered should oppose the zero curvature of the smectic layer. However, it is well-known from theoretical polymer conformation studies that squeezing a polymer chain between two walls does not induce any type of transverse spatial periodic modulation [103]. Therefore, this first explanation cannot hold. A second possible explanation is that the packing density of the mesogenic cores within a smectic layer may be different from that of the backbone segments. This would create an intrinsic frustration depending on the type of random walk performed by the backbone. The modulation would then appear to relieve this frustration in a similar way as that of the Skoulios pinches in discotic columnar phases [104]. This hypothesis could be checked by studying the influence on the layer undulations, of the mesogenic core grafting density on the backbone.

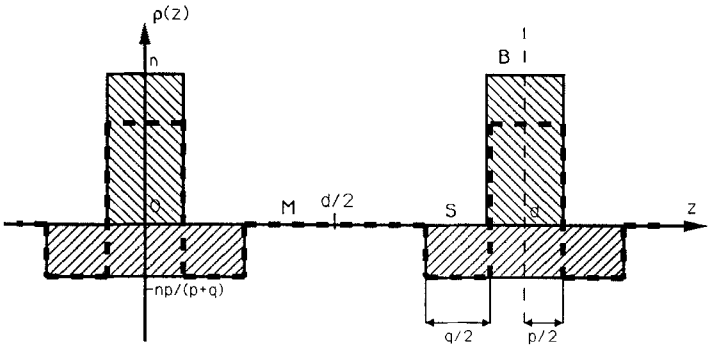

Figure 22. Representation of the electronic density in terms of step functions inside the unit cell, i.e. the smectic layer. X-rays being only sensitive to the contrast, the electron density of the mesogenic cores has been arbitrarily assigned to zero. Since we do not make absolute intensity measurements and since we deal with a purely displacive disorder, the backbones and the (spacers plus end chains) have been represented by two different step functions of equal hatched areas. The resulting electron density profile is shown as a thick broken line. M, S and B stand for the mesogenic core, spacer plus end chain and backbone regions, respectively.

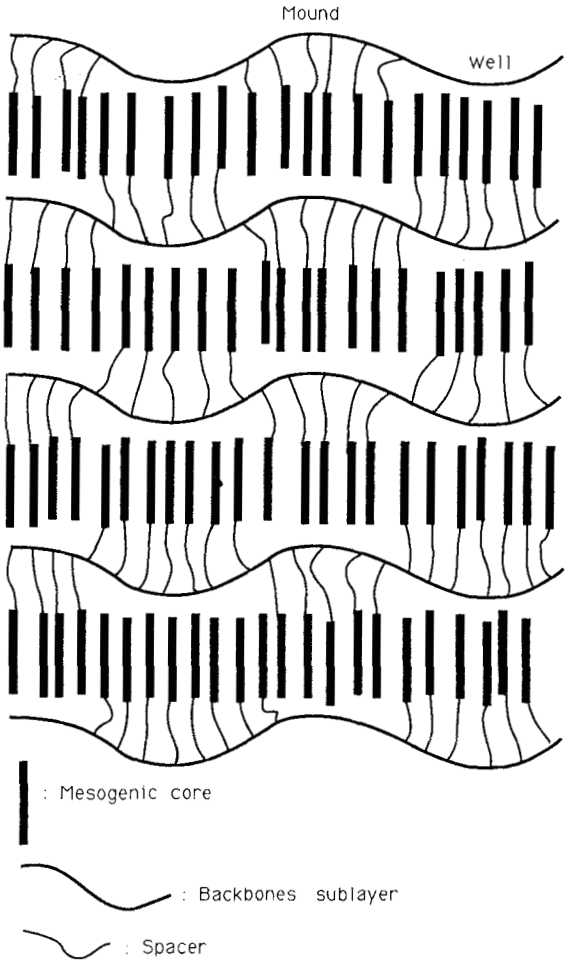

Figure 23. A two dimensional cut of the undulation local order schematic picture. Only a part of the smectic layer undulates, i.e. the backbones and the spacers. The end chains have been omitted for clarity. The layer undulations induce mound and well regions where the spacers adopt a splay-like configuration.

The S_B phase may also have layer undulations: looking at the X-ray diffraction pattern of the $P_{3,8}$ polysiloxane in its S_B phase (see figure 24), the whole row of the $10l$ diffuse spots may be seen. Their intensities follow the structure factor governing the Bragg reflections which shows that the whole layer undulates. That was also the case for the S_A phase of this polymer. The interesting phenomenon is that, on decreasing the temperature, whereas the layer undulation period a hardly varies in the S_A phase, it suddenly jumps to a definite value a_B at the S_A–S_B phase transition and it then remains constant. This period a_B, though being ill-defined since the undulation is only a short range ordering process, is roughly equal to twice the distance between the densest rows $[h0]$ of the two dimensional hexagonal lattice. Thus, there appears a kind of lock-in of the layer undulation period on that of the hexagonal lattice. This situation is depicted in figure 25 where mesogenic cores alternately displaced in the $+z$ and $-z$ directions are represented. In the case of the S_B phase, we can deduce more information

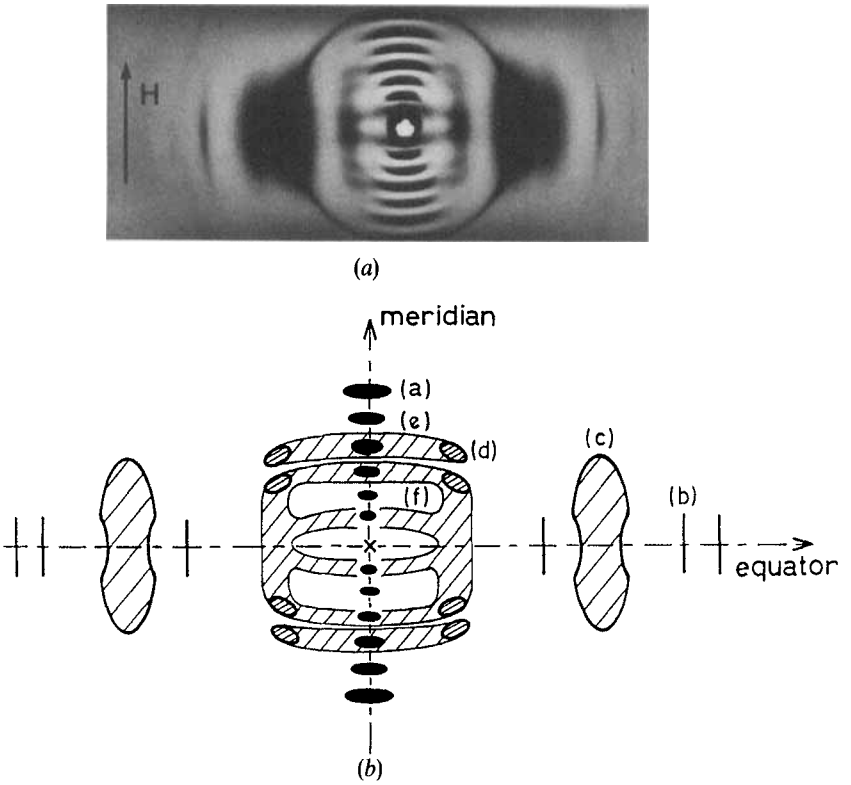

Figure 24. (*a*) Over exposed X-ray diffraction pattern of polymer $P_{3,8}$ in the S_B phase. *H* is the magnetic field direction. (*b*) Schematic representation of (*a*). a, (00*l*) reflections on the smectic layers; b, (100), (110) and (200) hexagonal lattice reflections within each smectic layer; c, large equatorial diffuse spot which is actually split along the meridian; d, (1/2 0 l) diffuse spots; e, diffuse streaks; f, curved diffuse streaks.

about the in-plane undulation symmetry: this symmetry cannot be hexagonal because such a distribution of up and down displacements on a hexagonal lattice would induce an intrinsic frustration. Therefore, the undulation symmetry can only be locally rectangular. The polymeric nematic phase may also display these kinds of diffuse spots, though quite smeared, if it has smectic fluctuation of a correlation length larger than the undulation period.

The case where diffuse spots exist but are not located in the same (00*l*) reciprocal planes as the Bragg spots (see figure 26) is much more difficult to explain and to represent. Clearly, some type of displacive layer modulation involving the backbones is relevant. However this modulation cannot be purely transverse and the way it can be accommodated with the smectic periodicity is still an open question.

Finally, let us remark that when an aligned polymeric mesophase crystallizes, the diffuse spots usually condense and their intensity strongly increases while other Bragg spots appear. Therefore it seems that the vectors of the crystalline three-dimensional lattice are closely related to the undulation wavevectors. This supports our point of view that the diffuse spots are due to a transverse modulation of the layers. In some way, this also supports the approach of Zugenmaier *et al.* [41] which aims at obtaining structural information about the mesophase from the study of crystalline fibres.

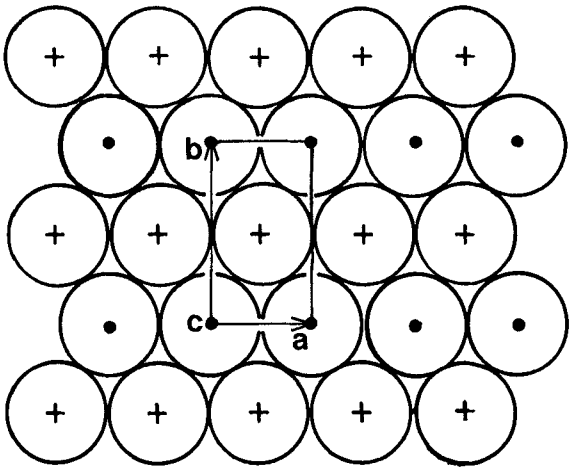

Figure 25. Layer undulation wavevector lock-in upon the hexagonal lattice parameter. The undulation short range order locally breaks the hexagonal symmetry and the organization can be described by a rectangular cell shown with $b = a\sqrt{3}$. Mesogenic cores displaced in the $+z$ direction are labelled with a filled disc whereas mesogenic cores displaced in the $-z$ direction are labelled with a cross.

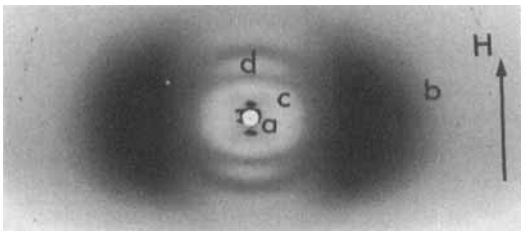

Figure 26. Overexposed X-ray diffraction pattern of polymer $P_{4,1}$ in the S_A phase. a, Bragg reflections; b, wide angle diffuse ring; c, diffuse spots which are not located in the same reciprocal planes as the smectic Bragg spots; d, curved diffuse streaks due to intramolecular interferences, H is the magnetic field direction.

3.3. *Fluctuations of $S_{\tilde{A}}$ symmetry*

By carefully inspecting the X-ray diffraction pattern of the polymer $PMAOC_4H_9$ (see figure 18(*b*)), additional small weak diffuse spots (e) may be noticed. They are located in special positions: (1/2, 0, 1/2) and (1/2, 0, 3/2) of the lattice built with **a** and **d**. This is indicative of superstructure $2\mathbf{a} \times 2\mathbf{d}$ characteristic of the $S_{\tilde{A}}$ phase which is sometimes found in the polymorphism of conventional polar mesogens [85]. The molecular organization in this phase can be described in terms of an antiferroelectric ordering on a two dimensional centred lattice. We can orient a given mesogenic core by considering the end by which it is grafted. Thus, the mesogenic cores may be represented by arrows which allows a schematic picture (see figure 27) of the polymeric $S_{\tilde{A}}$ phase to be drawn. The density of the backbone sublayer should be modulated with periods $2\mathbf{d}$ and $2\mathbf{a}$.

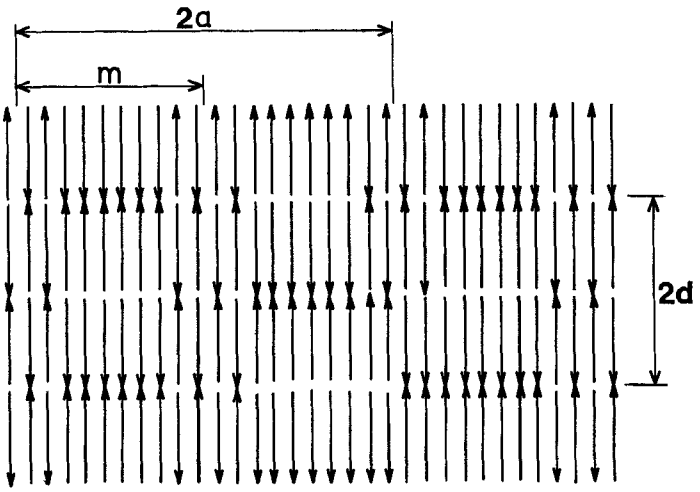

Figure 27. The molecular organisation in the $S_{\tilde{A}}$ phase: molecules in the case of 'conventional' mesogens or side chains in the case of comb-like polymers are represented by arrows. The $S_{\tilde{A}}$ phase is a modulated two dimensional fluid phase which can be described by an up-down ordering broken by antiphase walls organized in a periodic way. The period ($2d$) along the director is twice the thickness of a basic smectic lever; the distance between antiphase walls is m. The phase can be described by a two dimensional centred rectangular lattice.

Mesomorphic polymers deuteriated in the backbone are usually needed in order to perform small angle neutron scattering experiments and their X-ray diffraction patterns are generally similar to those of their protonated counterparts. However the same polymethacrylate, deuteriated in the backbone PMA(D)OC_4H_9, has a slightly different X-ray diffraction pattern [84] because the diffuse spots (e) become diffuse streaks perpendicular to the director. This means that the correlation length in the direction parallel to the layers is much smaller and shows that the rigidity of the backbone should indeed play a role in this type of ordering. In this system, the $S_{\tilde{A}}$ fluctuations are very weak and their correlation lengths are rather small (≈ 100 Å). However, mesomorphic combined polymers (polymers which have mesogenic cores as side chains and also within the backbones) may present this type of ordering over a long range resulting in a true $S_{\tilde{A}}$ phase [105]. The same kind of antiferroelectric ordering can also occur in the S_C phase and the corresponding $S_{\tilde{C}}$ phase has already been observed in conventional systems [85]. Several new chiral mesomorphic comb-like polymers also exhibit X-ray diffraction patterns characteristic of this type of ordering [106].

3.4. *Herring bone lattice fluctuations in the polymeric S_B phase*

In the conventional S_B phases, the molecules are located on a hexagonal lattice and are usually subjected to a short range order of lower (rectangular) symmetry called herring bone lattice fluctuations [95, 107] (see figure 28): the hexagonal lattice may also be described by a centred rectangular cell of vectors **a** and **b** with $b = a\sqrt{3}$. The effect of this short range order is to make the positions at the centre and at the corners of the rectangular cell no longer equivalent. It usually has a correlation length of about 20 Å inside the layers and is completely uncorrelated between adjacent layers. It then gives rise to a diffuse scattering in particular positions of reciprocal space, and therefore to

diffuse spots in the X-ray diffraction patterns. In fibre samples of uniaxial symmetry, these diffuse spots become a torus which is located in the equatorial plane and which has the meridian for the axis. The over exposed X-ray diffraction pattern (see figure 24) of the polymeric S_B phase also has such diffuse spots which shows that the herring bone lattice fluctuations also exist in polymeric systems. However, these diffuse spots do not have exactly the same appearance as that displayed by conventional mesogens because they are slightly split off from the equator [10]. This means that these fluctuations are now slightly correlated along the meridian between adjacent layers. This situation is shown in figure 29 where the rectangular unit cell of the herring bone lattice is depicted. The ellipses represent the cross sections of the side chains perpendicular to their long

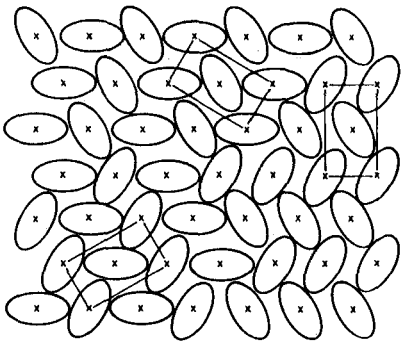

Figure 28. Herring bone lattice fluctuations within the layers of the 'conventional' S_B phase. The ellipses represent the cross sections of the molecules and the crosses their centres of gravity. The long range hexagonal symmetry is locally broken and domains of rectangular symmetry appear with three different kinds of orientation.

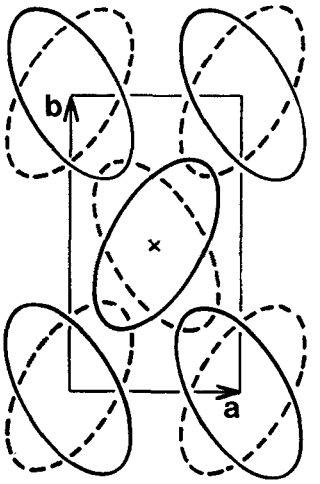

Figure 29. Correlations of the herring bone lattice fluctuations among adjacent layers in the 'polymeric' S_B phase. The solid line ellipses are the sections of the mesogenic cores located in a given layer; the dashed line ellipses are the sections of the mesogenic cores located in the two adjacent layers.

axis. The solid line ellipses correspond to side chains located in a given layer whereas the dashed line ellipses correspond to side chains located in the two neighbouring layers. Projected on the $z=0$ plane, the density is again equivalent to that of a hexagonal lattice which should suppress the diffuse intensity on the equator and transfer it essentially to the $s_z = \pm 1/d$ reciprocal planes. Of course, the organization depicted in figure 29 is ideal whereas we only observe a tendency for such an order and moreover over a short range. Nevertheless, this again illustrates the idea that though the backbones prevent the establishment of a true crystalline long range order in the S_B phase, they rather enhance the short range order among neighbouring mesogenic cores.

Finally we conclude by recalling that two short range orders of the same symmetry may interact. For instance, the herring bone fluctuations and the layer undulations in the polymeric S_B phase are of the same rectangular symmetry so that we can imagine that the mesogenic cores lying at the corners of the rectangular cells of figure 29 are displaced in the $+z$ direction while those lying at the centres of the cells are displaced in the $-z$ direction by the layer undulations.

4. Localized defects

In addition to the X-ray diffuse scattering described in the previous section, some additional intensity may also be detected in several X-ray diffraction patterns of mesomorphic comb-like polymers. This additional diffuse intensity cannot be explained in terms of collective fluctuations but rather in terms of localized defects such as edge dislocations, for example. We have used two ways to deal with the diffraction by such objects: the first consists in considering a sketch of the defect and a direct analytic computation of the diffraction pattern. The second consists in reducing the same sketch on to a slide. This slide is then placed on the path of a He–Ne laser beam and the resulting diffraction pattern is observed using a simple optical set-up. This optical diffraction pattern can then be compared with the X-ray one and the sketch of the defect may be modified in order to fit the X-ray pattern better. Of course, this optical diffraction method is in no way restricted to the analysis of localized defects in the mesophases and it has been already widely used [108]. We shall now illustrate this method by two examples of defects disturbing the polymeric S_A mean structure. The first describes defects related to the crossing of the smectic layers by the backbones and the second describes edge dislocations.

4.1. *Layer crossing by the backbones*

The X-ray diffraction pattern shown in figure 18 (*b*) displays some very unusual diffuse scattering (f) which we have called moustaches [7]. This diffuse scattering is of very low intensity, barely larger than the noise. It is located around the strongest Bragg reflections which implies that the mean layered structure is affected. Oddly enough, the moustaches are not centrosymmetric around the Bragg spots; this implies a peculiar internal structure inside the defects. Moreover the Bragg spots remain resolution limited (with our X-ray equipment) so that the smectic layers are still continuous. To account for the existence of this diffuse scattering, we assume that the defects are randomly distributed so that they do not diffract coherently. Since the moustaches are inclined at an angle θ with respect to the meridian, then the defects must also be inclined by the same angle with respect to the director of the S_A matrix (see figure 30); these defects must therefore be biaxial. However, because of the uniaxial symmetry of the sample, it is difficult to estimate their two widths independently. In particular, it is difficult to tell whether the defects which give rise to the moustaches are linear defects or

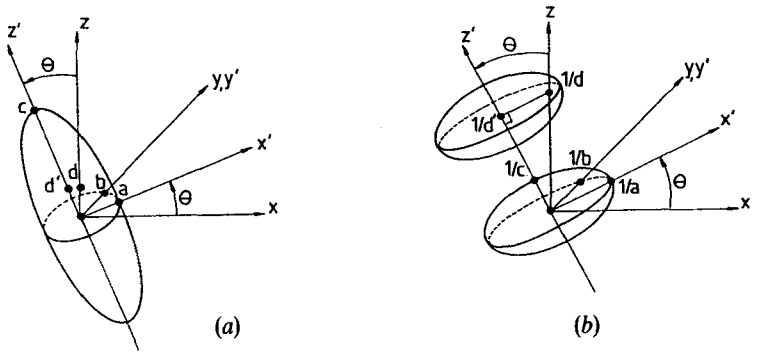

Figure 30. (*a*) A picture in direct space of the defect as an ellipsoid of radii *a*, *b* and *c*, tilted by an angle θ with respect to the normal Oz to the smectic layers. (*b*) Corresponding diffusion domains in reciprocal space.

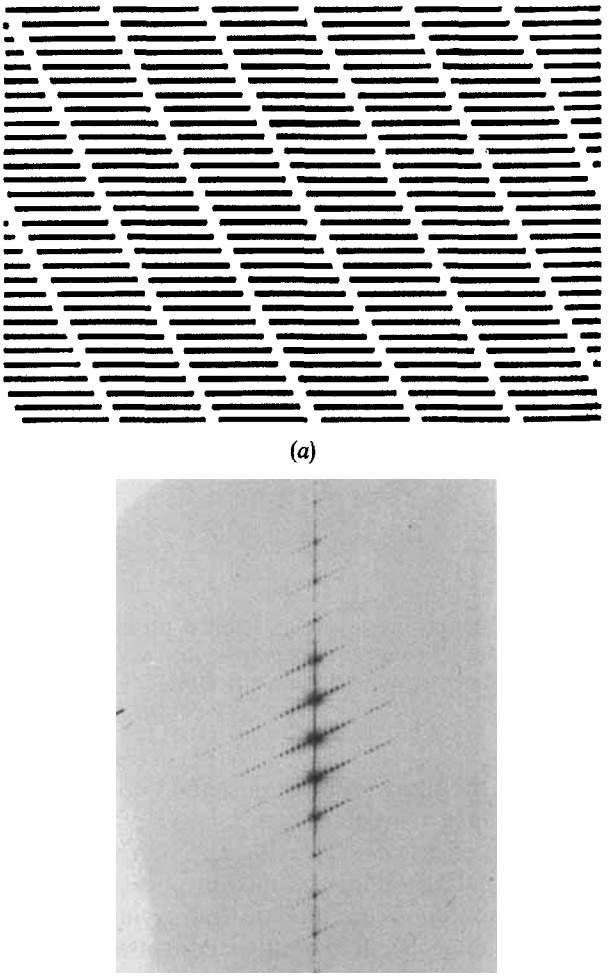

(*a*)

(*b*)

Figure 31. (*a*) A sketch of defects displaying no internal structure, i.e. nematic regions. (*b*) Corresponding optical diffraction pattern. Diffuse streaks appear around the Bragg reflections but they are centrosymmetric around them. (The streaks are modulated because the defects are equally spaced.)

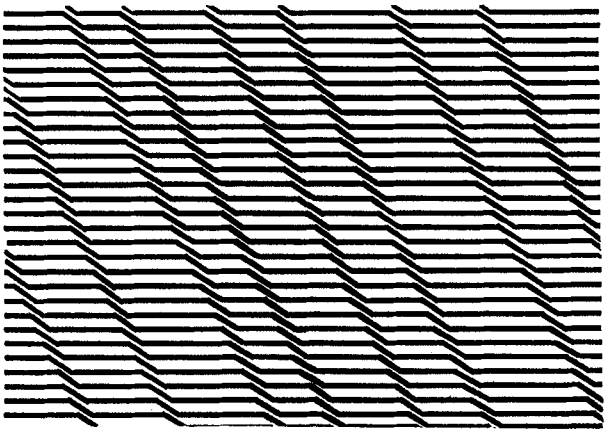

(*a*)

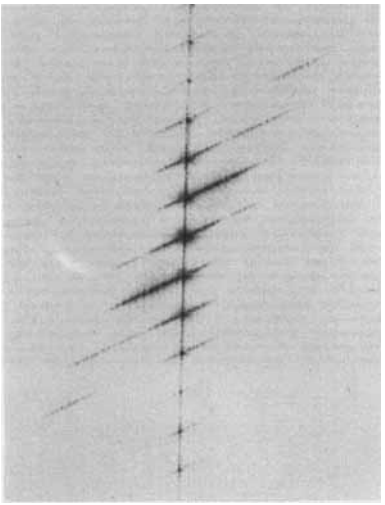

(*b*)

Figure 32. (*a*) A sketch of defects displaying an internal periodicity. (*b*) The corresponding optical diffraction pattern. Diffuse streaks may be seen around the Bragg reflections but they are not centrosymmetric around them any more.

wall defects [7]. However, the optical diffraction method works only in two dimensions and so only a projection of the molecular organization on to a plane may be obtained. Figure 31 shows a sketch of defects displaying no internal structure (i.e. a nematic region) and the corresponding optical diffraction pattern. Diffuse streaks indeed appear around the Bragg reflections but they are centrosymmetric around them. Some kind of diffracting pattern must therefore be introduced inside the defect as is shown in figure 32. In this case the optical diffraction pattern is really similar to that of the X-ray experiment.

At this point, it is now convenient to compute analytically the diffraction by the sketch shown in figure 32 and check that it can actually describe the X-ray diffraction pattern observed. To perform this calculation, the object is represented in figure 33 by

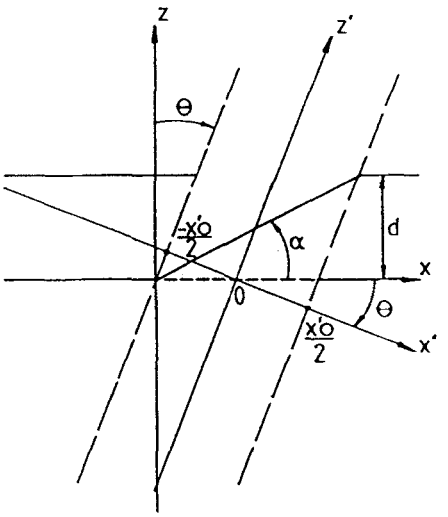

Figure 33. Defect scheme used for the calculations. Dashed line: missing portion of a smectic layer; solid line: tilted segment which represents the defect internal structure. x'_0 is the apparent width of the defect.

suppressing the horizontal part of a layer (the dashed line) and replacing it by another straight line segment (the solid line). The equations for the two segments are

$$-\frac{x'_0}{2}<x'<\frac{x'_0}{2}, \quad z'=x'\tan\theta$$

$$-\frac{x'_0}{2}<x'<\frac{x'_0}{2}, \quad z'=x'\left(\tan\theta+\frac{d}{x'_0\cos\theta}\right)+\frac{d}{2\cos\theta},$$

where d is the smectic period, x'_0 is the average width of the defect and (x', z') is a system of rectangular axes attached to the defect. The scattered intensity around the first Bragg reflection is given by

$$I(s_{x'})=\frac{\sin^2\pi x'_0[s_{x'}+(\sin\theta/d)]}{x'^2_0\pi^2[s_{x'}+(\sin\theta/d)+1/x'_0]^2\,[s_{x'}+(\sin\theta/d)]^2}.$$

It can be shown [7] that this scattered intensity is indeed not symmetric around the Bragg spots. The average width x'_0 of the defect represents the only fit parameter and its value is adjusted to about 20 ± 5 Å. It remains to give a physical interpretation to the defect shown in figure 32 (*a*). We recall here the small angle neutron scattering results obtained on the same polymer [62]: the gyration radii of the backbone along the director $R_{\|}$ and perpendicular to it $R_{\perp}$ have been measured and the values $R_{\|}=22\pm3$ Å and $R_{\perp}=86\pm9$ Å obtained. However, by inspecting the electron density profile (see figure 10 (*c*)) obtained using the procedure described in § 2, it can be seen that the backbone is essentially located in a region at most 10 Å wide along the director. The smectic period being here equal to $29{\cdot}5\pm0{\cdot}5$ Å, this means that the backbone should sometimes hop from a smectic layer to an adjacent one and this, on average, about once per coil. Such layer hopping by the chains has already been predicted theoretically [109] and would create defects which may interact and build up the objects depicted in

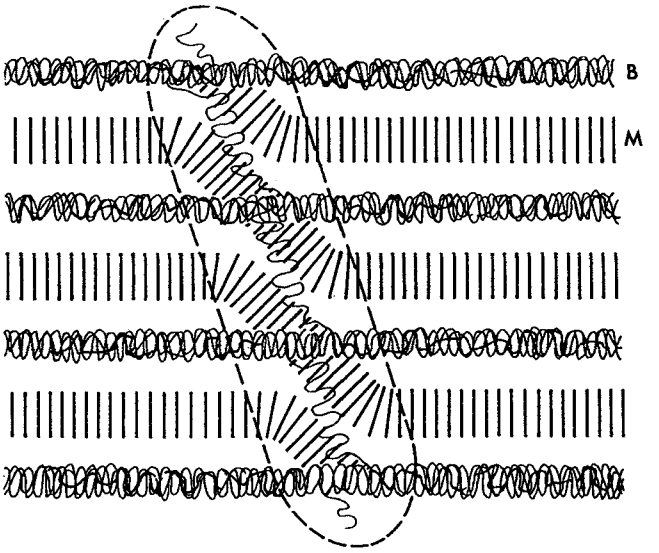

Figure 34. Interpretation of the defect represented in figure 32 (*a*) in terms of layer hopping by the backbones. B, backbones sublayer; M, mesogenic cores sublayer; dashed line, limits of the defect. The spacers and end chains have been omitted for clarity.

figure 34. Such objects would indeed look very much like the defect shown in figure 32 (*a*) and can therefore account for the moustaches. In that case, the ratio of this diffuse scattering to the Bragg reflection intensities may be estimated [7] and is in good agreement with experiment. This supports our hypothesis that the objects detected through their contribution to the X-ray diffraction pattern are indeed related to the crossing of the smectic layers by the backbones.

4.2. *Edge dislocations*

We now return to the cyanosubstituted mesomorphic polyacrylate P_n series presented in § 2.2.2. The over exposed X-ray diffraction pattern of polymer P_8 is shown in figure 35. A diffuse scattering (c) is visible in addition to the Bragg reflections (a) and the wide angle diffuse crescents (b). This diffuse scattering has a very low intensity and because of its special shape, we have called it 'butterfly wings' [12]. The existence of the butterfly wings may be explained by the presence in the S_A phase of edge dislocations. Within the framework of the elastic continuum theory, the deformation field of an edge dislocation in a lamellar phase is already well known [110, 111]. This field depends on a typical length λ defined by $\lambda=(K_1/B)^{1/2}$ where K_1 and B are the elastic constants for splay and compression of the layers, respectively. The distorted region is essentially located inside the parabola $z=\lambda^{-1}x^2$ (see figure 36). Knowledge of the elastic deformation field allows us to draw sketches for optical diffraction experiments. Such a sketch for $\lambda/d=0{\cdot}03$ where $d=48$ Å is the smectic period, and its corresponding optical diffraction patterns are shown in figure 37. The characteristic curves (C) and (C') which limit the X-ray diffuse scattering and make it appear as 'butterfly wings' can only be guessed on over exposed optical patterns. Actually the noise probably due to the laser speckle seriously limits the optical diffraction experiments compared to those with X-rays. However microdensitometric recordings show that the optical pattern fits the X-ray one for the value $\lambda/d\approx 0{\cdot}030\pm 0{\cdot}015$.

The analytical calculation of the Fourier transform of the elastic deformation field can also be made [12]. The elastic deformation field may be expressed in the form [110]

$$u_n(x)=\frac{d}{4}+\frac{d}{4\pi}\int\frac{dq}{iq}\exp(iqx)\exp(-nd\lambda q^2)$$

and the Fourier transform will be described by

$$A'\left(s_{x'}\frac{p}{d}+\delta s_z\right)\approx\frac{pF(p/d)}{s_x}\frac{4\pi^2\lambda d s_x^2}{4\pi^2(\delta s_z)^2d^2+(4\pi^2\lambda d s_x^2)^2}$$

which when squared represents the diffuse scattering intensity at wavevectors $(s_x, \delta s_z)$ around the Bragg reflection of order p and structure factor $F(p/d)$. The fact that the 'butterfly wings' may only be seen around the third order Bragg reflections comes partly from the influence of the prefactor p in these formulae for the scattered amplitude and partly because the diffuse scattering follows the peculiar structure factor $F(p/d)$ of the smectic layers (see § 2.2.2). The isointensity lines and curves (C) and (C') can also be calculated and compared to experiment. The only fit parameter is λ and the value obtained $\lambda=1{\cdot}2\pm0{\cdot}6$ Å agrees well with that derived from the optical diffraction method. Therefore, the 'butterfly wings' may well be explained by the presence of edge dislocations in this polymeric S_A phase. Actually, edge dislocations have already been

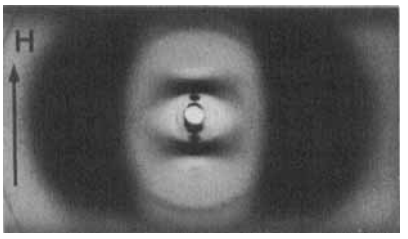

(*a*)

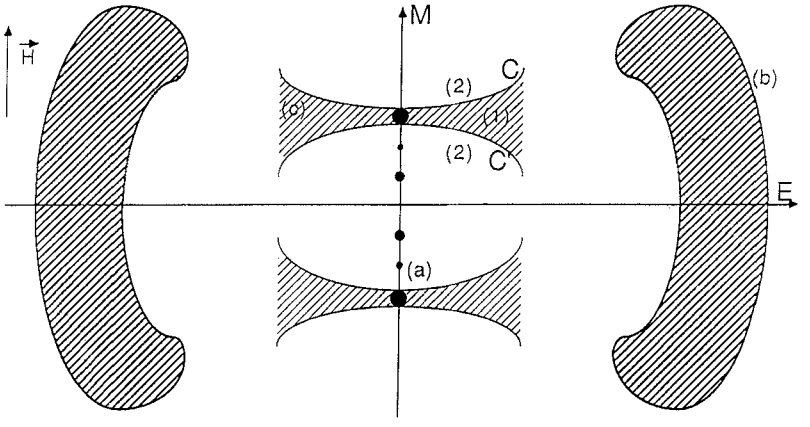

(*b*)

Figure 35. (*a*) Over exposed X-ray diffraction pattern of the cyanosubstituted P_8 polyacrylate in the S_A phase. *H* is the magnetic field direction. (*b*) Schematic representation of (*a*). a, Bragg reflections; b, wide angle diffuse ring; c, diffuse streaks called butterfly wings; Parabolae (C) and (C') are essentially contrast lines which separate region (1) of stronger scattering from the background (2). M and E stand for meridian and equator, respectively.

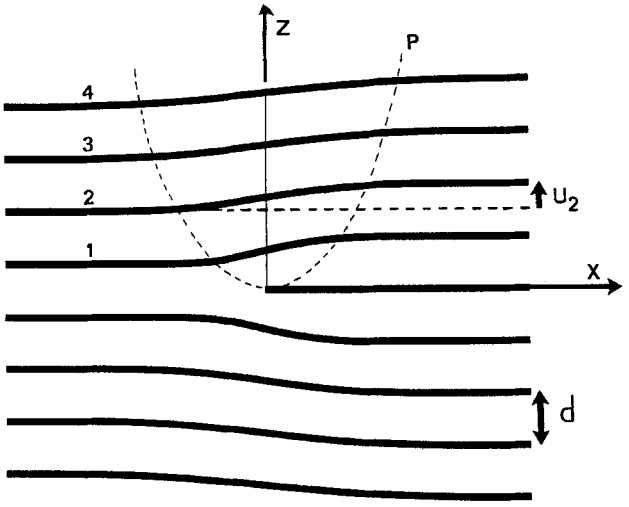

Figure 36. A sketch of an edge dislocation in a smectic phase. d is the smectic period and u_2 is the displacement of layer number 2. The elastic distortion field is located inside a parabola P of curvature $\lambda^{-1}=(B/K)^{1/2}$ where K and B are the elastic constants for splay and compression of the layers, respectively.

directly observed by electron microscopy in 'combined' liquid crystal polymers [66].

Several orders of magnitude should now be discussed: first the length λ is of the order of a few Å whereas it is usually a few tens of Å for conventional mesogens. The splay elastic constant K_1 of a few mesomorphic comb-like polymers have already been measured [112, 113] and were found to be of the same order of magnitude as those of conventional mesogens. Since $\lambda=(K_1/B)^{1/2}$, then the elastic constant B for compression of the layers should be about 100 times larger for a polymeric S_A phase than for a conventional one. Indeed the high resolution X-ray study done by Nachaliel *et al.* [59] shows that B may be extrapolated to large values away from the S_A–N phase transition. It should also be recalled here that the smectic layer thermal fluctuation modes cannot usually be detected in the X-ray diffraction patterns of polymeric smectic phases. This indicates a change in their wavelengths and therefore *a priori* different orders of magnitude for the elastic constants B of polymeric mesophases compared to the conventional ones. The relatively large value of the elastic constant B may be explained by the intrinsic rigidity of the backbone sublayer and also by the fact that the permeation effect [114] in comb-like polymers also involves the diffusion of the backbone.

The dimensions of the core of the edge dislocations were inferred to be very small, no larger than 10 Å [12]. A similar situation was also observed by electron microscopy in germanium [115]. Finally, the ratio of the diffuse scattering to the Bragg reflection intensities was estimated and leads to a value for the edge dislocation density $n\approx 10^8\,\mathrm{cm}^{-2}$. This value can be compared to the values of 10^4–$10^6\,\mathrm{cm}^{-2}$ for good crystals, of 10^{10}–$10^{12}\,\mathrm{cm}^{-2}$ for laminated metals [116] and $10^9\,\mathrm{cm}^{-2}$ for screw dislocations of some lyotropic lamellar phases [117]. Thus, fairly large dislocation densities are needed in order to observe their contribution to the X-ray diffraction pattern.

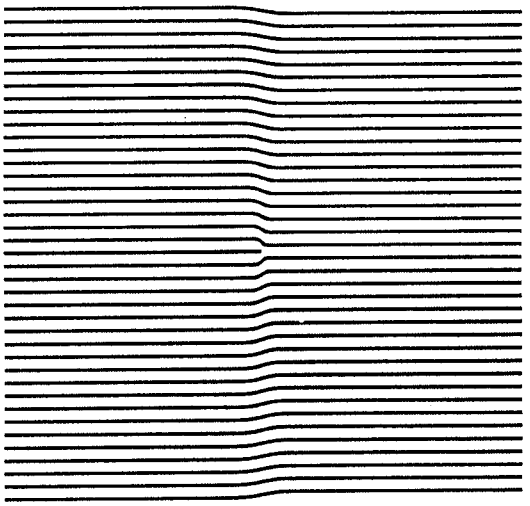

(*a*)

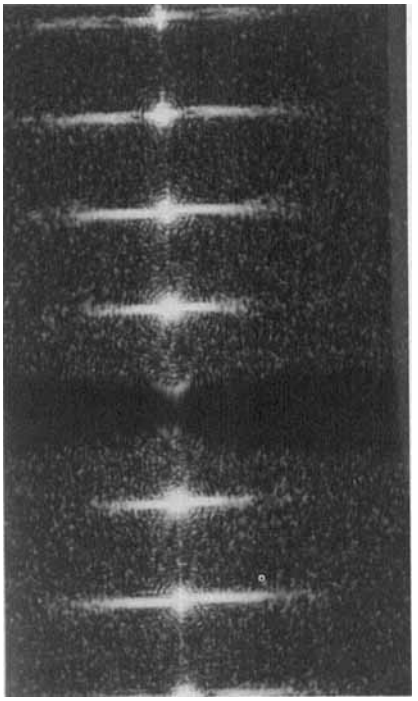

(*b*)

Figure 37. (*a*) A computer drawing of the elastic deformation field of an edge dislocation in a smectic phase for λ/d of 0·03. (*b*) The corresponding optical diffraction pattern.

5. Conclusion

X-ray diffraction is a powerful tool for characterization and mesophase identification but it can also give much more information about the molecular organization of these phases. The study of the different (orientational, positional, etc.) kinds of long range order not only helps to determine the mesophase symmetry but also by exploiting the diffraction intensities, allows us to probe the density distribution. Thus, the localization of the backbone in the polymeric smectic phases could be studied: for some comb-like polymers, it was shown that the backbones are rather well-confined in sublayers of the smectic layers whereas the backbones of other comb-like polymers hardly feel the smectic field. Whether this behaviour is related to the mesophase compressibility is still an interesting and open question. So are the problems of the absolute intensities of reflection from the smectic layers and of the comparison of the smectic period d with the side chain length l. In addition, high resolution X-ray equipment helps us to study the correlation length of the pretransitional fluctuations and check to which extent they can be described by theory. They can also reveal the limitations imposed by the presence of the backbones upon the long range order.

The X-ray diffuse scattering out of the Bragg reflections has received yet very little attention in the field of mesomorphic comb-like polymers. However this diffuse scattering can give interesting information about the possible short range order which may affect the average organization determined by using the Bragg reflections. We have shown that these polymers do indeed display various kinds of short range order and are, therefore, good examples with which to illustrate these ideas. The most striking example is perhaps that of the layer undulations though their physical origin is not yet clear. Further experiments involving partially grafted polymers may help to explain this point. The diffuse X-ray scattering can also give information about defects such as dislocations which may be important to understand rheological experiments. However, since the defects do not scatter coherently, small defect densities will not be detected.

Let us now try to summarize the influence of the backbone upon the organization in the polymeric mesophases. It seems that since the backbone, for entropic reasons, naturally tries to reach the most disordered state possible, then it tends to lessen the strength and even sometimes the correlation length of the positional long range order. It can also create defects such as layer hopping to escape the confinement imposed by the smectic field. On the other hand a given backbone induces correlations between the neighbouring mesogenic cores chemically linked to it and therefore strongly promotes various kinds of short range order. The influence of the backbone tacticity on this effect would be quite interesting to study. Thus, X-ray diffraction experiments show how the backbones of mesomorphic comb-like polymers actually play a subtle part.

It is for us a pleasure to thank the chemists: the Bordeaux liquid crystal group of the CRPP Laboratory, P. Keller, G. Scherowsky, L. Strzelecki and the liquid crystal group of the Thomson Company who kindly provided us with the samples and with whom we had many fruitful discussions.

References

[1] STRZELECKI, L., and LIÉBERT, L., 1973, *Bull. Soc. Chim.*, **2**, 597 and references therein.
[2] FINKELMANN, H., RINGSDORF, H., and WENDORFF, J. H., 1978, *Makromolek. Chem.*, **179**, 273.

[3] For a general outline of the field of side chain liquid crystal polymers, see McArdle, C. B. (editor), 1989, *Side Chain Liquid Crystal Polymers* (Blackie). For a review of the chemical syntheses of side chain liquid crystal polymers, see PERCEC, V., and PUGH, C., *Ibid.*, chap. 2, GRAY, G. W., *Ibid.*, chap. 3.
[4] DAVIDSON, P., KELLER, P., and LEVELUT, A. M., 1985, *J. Phys., Paris*, **46**, 939.
[5] DAVIDSON, P., 1984, Ph.D. Thesis, Université de Paris Sud-Orsay, France.
[6] DECOBERT, G., SOYER, F., DUBOIS, J. C., and DAVIDSON, P., 1985, *Polymer Bull.*, **14**, 549.
[7] DAVIDSON, P., and LEVELUT, A. M., 1988, *J. Phys, Paris*, **49**, 689.
[8] DAVIDSON, P., and STRZELECKI, L., 1988, *Liq. Crystals*, **3**, 1583.
[9] DAVIDSON, P., LEVELUT, A. M., ACHARD, M. F., and HARDOUIN, F., 1989, *Liq. Crystals*, **4**, 561.
[10] DAVIDSON, P., and LEVELUT, A. M., 1989, *J. Phys. Paris*, **50**, 2415.
[11] SCHEROWSKY, G., MÜLLER, U., SPRINGER, J., TRAPP, W., LEVELUT, A. M., and DAVIDSON, P., 1989, *Liq. Crystals*, **5**, 1297.
[12] DAVIDSON, P., PANSU, B., LEVELUT, A. M., and STRZELECKI, 1991, *J. Phys. II, Paris*, **1**, 61.
[13] NOËL, C., 1989, *Side Chain Liquid Crystal Polymers*, edited by C. B. McArdle (Blackie), chap. 6 and references therein.
[14] DURAN, R., GUILLON, D., GRAMAIN, P., and SKOULIOS, A., 1987, *Makromolek. Chem. Commun.*, **8**, 181.
[15] DURAN, R., GUILLON, D., GRAMAIN, P., and SKOULIOS, A., 1987, *Makromolek. Chem. Rap. Commun.*, **8**, 321.
[16] DURAN, R., GUILLON, D., GRAMAIN, P., and SKOULIOS, A., 1987, *J. Phys., Paris.* **48**, 2043.
[17] DURAN, R., GUILLON, D., GRAMAIN, P., and SKOULIOS, A., 1988, *J. Phys., Paris*, **49**, 1455.
[18] FRÈRE, Y., YANG, F., GRAMAIN, P., GUILLON, D., and SKOULIOS, A., 1988, *Makromolek. Chem.*, **189**, 419.
[19] MAUZAC, M., HARDOUIN, F., RICHARD, H., ACHARD, M. F., SIGAUD, G., and GASPAROUX, H., 1986, *Euro. Polymer J.*, **22**,137.
[20] SHIBAEV, V. P., KOSTROMIN, S. G., and PLATE, N. A., 1982, *Euro. Polymer J.*, **18**, 651.
[21] TALROZE, R. V., SINITZYN, V. V., SHIBAEV, V. P., and PLATE, N. A., 1982, *Molec. Crystals Liq. Crystals*, **80**, 211.
[22] KOSTROMIN, S. G., SINITZYN, V. V., TALROZE, R. V., SHIBAEV, V. P., and PLATE, N. A., 1982, *Makromolek. Chem. Rap. Commun.*, **3**, 809.
[23] TSUKRUK, V. V., LOKHONIA, O. A., SHILOV, V. V., KUZMINA, V. A., and LIPATOV, YU. S., 1983, *Makromolek. Chem. Rap. Commun.*, **4**, 595.
[24] KONSTANTINOV, Y. B., AMERIK, Y. B., ALEKSANDROV, A. I., and PASHKOVA, T. V., 1984, *Molec. Crystals Liq. Crystals*, **110**, 121.
[25] FREIDZON, YA. S., BOIKO, N. I., SHIBAEV, V. P., TSUKRUK, V. V., SHILOV, V. V., and LIPATOV, YU. S., 1986, *Polymer*, **27**, 190.
[26] FREIDZON, YA., S., TALROZE, R. V., BOIKO, N. I., KOSTROMIN, S. G., SHIBAEV, V. P., and PLATE, N. A., 1988, *Liq. Crystals*, **3**, 127.
[27] GEMMELL, P. A., GRAY, G. W., LACEY, D., ALIMOGLU, A. K., and LEDWITH, A., 1985, *Polymer*, **26**, 615.
[28] SUTHERLAND, H. H., BASU, S., and RAWAS, A., 1987, *Molec. Crystals Liq. Crystals*, **145**, 73.
[29] SUTHERLAND, H. H., and RAWAS, A., 1986, *Molec. Crystals Liq. Crystals*, **138**, 179.
[30] SUTHERLAND, H. H., ALI ADIB, Z., GRAY, G. W., LACEY, D., NESTOR, G., and TOYNE, K. J., 1988, *Liq. Crystals*, **3**, 1293.
[31] LE BARNY, P., DUBOIS, J. C., FRIEDRICH, C., and NOËL, C., 1986, *Polymer Bull.*, **15**, 341.
[32] DECOBERT, G., DUBOIS, J. C., ESSELIN, S., and NOËL, C., 1986, *Liq. Crystals*, **1**, 307.
[33] ESSELIN, S., BOSIO, L., NOËL, C., DECOBERT, G., and DUBOIS, J. C., 1987, *Liq. Crystals*, **2**, 505.
[34] ZENTEL, R., and STROBL, G. R., 1984, *Makromolek. Chem.*, **185**, 2669.
[35] ZENTEL, R., SCHMIDT, G. F., MEYER, J., and BENALIA, M., 1987, *Liq. Crystal.*, **2**, 651.
[36] GILLI, J. M., FAUBERT, F., SIXOU, P., and LAÜGT, S., 1989, *Liq. Crystals*, **4**, 357.
[37] DIELE, S., HISGEN, B., RECK, B., and RINGSDORF, H., 1986, *Makromolek. Chem. rap. Commun.*, **7**, 267.
[38] DIELE, S., OELSNER, S., KUSCHEL, F., HISGEN, B., RINGSDORF, H., and ZENTEL, R., 1987, *Makromolek. Chem.*, **188**, 1993.
[39] KOSTROMIN, S. G., SHIBAEV, V. P., and DIELE, S., 1990, *Makromolek. Chem.*, **191**, 2521.
[40] GIESSELMANN, F., and ZUGENMAIER, P., 1989, *Liq. Crystals*, **5**, 1567.

[41] ZUGENMAIER, P., and MÜGGE, J., 1984, *Makromolek. Chem. rap. Commun.*, **5**, 11.
[42] HANS, K., and ZUGENMAIER, P., 1988, *Makromolek. Chem.*, **189**, 1189.
[43] ZUGENMAIER, P., and MENZEL, H., 1988, *Makromolek. Chem.*, **189**, 2647.
[44] SHILOV, V. V., TSUKRUK, V. V., BLIZNYUK, V. N., and LIPATOV, YU. S., 1982, *Polymer*, **23**, 484.
[45] GUDKOV, V. A., CHISTYAKOV, I. G., SHIBAEV, V. P., and VAINSHTEIN, B. K., 1982, *Sov. Phys. Crystallogr.*, **27**, 324.
[46] GUDKOV, V. A., 1984, *Sov. Phys. Crystallogr.*, **29**, 316.
[47] SHILOV, V. V., TSUKRUK, V. V., and LIPATOV, YU. S., 1984, *J. Polymer. Sci.*, **22**, 41.
[48] TSUKRUK, V. V., SHILOV, V. V., and LIPATOV, YU. S., 1985, *Sov. Phys. Crystallogr.*, **30**, 115.
[49] TSUKRUK, V. V., SHILOV, V. V., and LIPATOV, YU S., 1985, *Acta pol.* **36**, 403.
[50] TSUKRUK, V. V., SHILOV, V. V., and LIPATOV, YU. S., 1986, *Macromolecules*, **19**, 1308.
[51] GUDKOV, V. A., 1987, *Sov. Phys. Crystallogr.*, **31**, 686.
[52] TSUKRUK, V. V., SHILOV, V. V., LIPATOV, YU. S., MOGILEVSKII, L. YU., FREIDZON, YA. S., BOIKO, N. I., and SHIBAEV, V. P., 1988, *Sov. Phys. Crystallogr.*, **33**, 286.
[53] TSUKRUK, V. V., SHILOV, V. V., LOKHONIA, O. A., and LIPATOV, YU. S., 1987, *Sov. Phys. Crystallogr.*, **32**, 88.
[54] TSUKRUK, V. V., and SHILOV, V. V., 1990. *Polymer*, **31**, 1793.
[55] ALEXANDROVA, A. I., PASHKOVA, T. V., KRÜCKE, B., KOSTROMIN, S. G., and SHIBAEV, V. P., 1991, *J. Physique II, Paris*, **1**, 939.
[56] NACHALIEL, E., KELLER, E. N., DAVIDOV, D., ZIMMERMANN, H., and DEUTSCH, M., 1987, *Phys. Rev. Lett.*, **58**, 896.
[57] KELLER, E. N., NACHALIEL, E., DAVIDOV, D., and ZIMMERMANN, H., 1988, *Phys. Rev.* A, **37**, 2251.
[58] KELLER, E. N., HALFON, R., NACHALIEL, E., DAVIDOV, D., and ZIMMERMANN, H., 1988, *Phys. Rev. Lett.*, **61**, 1206.
[59] NACHALIEL, E., KELLER, E. N., DAVIDOV, D., and BOEFFEL, C., 1991, *Phys. Rev.* A, **43**, 2897.
[60] FAN, Z. X., BUCHNER, S., HAASE, W., and ZACHMANN, H. G., 1990, *J. Chem. Phys.*, **92**, 5099.
[61] RICHARDSON, R. M., and HERRING, N. J., 1985, *Molec. Crystals, Liq. Crystals*, **123**, 143.
[62] NOIREZ, L., forthcoming review paper and references therein, *Liq. Crystals* (to be submitted).
[63] DURST, H., and VOIGT MARTIN, I. G., 1986, *Makromolek. Chem. rap. Commun.*, **7**, 785.
[64] VOIGT MARTIN, I. G., and DURST, H., 1987, *Liq. Crystals*, **2**, 585.
[65] VOIGT MARTIN, I. G., and DURST, H., 1987, *Liq. Crystals*, **2**, 601.
[66] VOIGT MARTIN, I. G., DURST, H., RECK, B., and RINGSDORF, H., 1988, *Macromolecules*, **21**, 1620.
[67] VOIGT MARTIN, I. G., and DURST, H., 1989, *Macromolecules*, **22**, 168.
[68] VOIGT MARTIN, I. G., DURST, H., and KRUG, H., 1989, *Macromolecules*, **22**, 595.
[69] VOIGT MARTIN, I. G., KRUG, H., and VAN DYCK, D., 1990, *J. Phys. Paris*, **51**, 2347.
[70] For a review of dielectric spectroscopy, see HAWS, C. M., CLARK, M. G., and ATTARD, G. S., 1989, *Side Chain Liquid Crystal Polymers*, edited by C. B. McArdle (Blackie), chap. 7 and references therein.
[71] KRÜGER, J. K., PEETZ, L., SIEMS, R., UNRUH, H. G., EICH, M., HERMANN SCHÖNHERR, O., and WENDORFF, J. H., 1988, *Phys. Rev.* A, **37**, 2637.
[72] REYS, V., DORMOY, Y., GALLANI, J. L., MARTINOTY, P., LEBARNY, P., and DUBOIS, J. C., 1988, *Phys. Rev. Lett.*, **61**, 2340.
[73] BENGUIGUI, L., RON, P., HARDOUIN, F., and MAUZAC, M., 1989, *J. Phys. Paris*, **50**, 529.
[74] BOEFFEL, C., and SPIESS, H. W., 1989, *Side Chain Liquid Crystal Polymers*, edited by C. B. McArdle (Blackie), chap. 8 and references therein.
[75] MONNERIE, L., LAUPRÊTRE, F., and NOËL, C., 1988, *Liq. Crystals*, **3**, 1013.
[76] SCHLEICHER, A., MÜLLER, K., and KOTHE, G., 1989, *Liq. Crystals*, **6**, 489.
[77] VAN DER PUTTEN, D., SCHWENK, N., and SPIESS, H. W., 1989, *Liq. Crystals*, **4**, 341.
[78] MAUZAC, M., RICHARD, H., and LATIÉ, L., 1990, *Macromolecules*, **23**, 753.
[79] OULYADI, H., LAUPRÊTRE, F., MONNERIE, L., MAUZAC, M., RICHARD, H., and GASPAROUX, H.,1990, *Macromolecules*, **23**, 1965.
[80] CASQUILHO, J. P., ESNAULT, P., VOLINO, F., MAUZAC, M., and RICHARD, H., 1990, *Molec. Crystals liq. Crystals*, **180B**, 343.
[81] CASQUILHO, J. P., and VOLINO, F., 1990, *Molec. Crystals liq. Crystals*, **180B**, 357.
[82] DE GENNES, P. G., 1974, *The Physics of Liquid Crystals* (Clarendon Press).

[83] BLINOV, L. M., BAIKALOV, V. A., BARNIK, M. I., BERESNEV, L. A., POZHIDAYEV, E. P., and YABLONSKY, S. V., 1987, *Liq. Crystals*, **2**, 121.
[84] DAVIDSON, P., and LEVELUT, A. M., (unpublished results).
[85] HARDOUIN, F., LEVELUT, A. M., ACHARD, M. F., and SIGAUD, G., 1983, *J. Chim. Phys. Physicochim. Biologique*, **80**, 53.
[86] LEADBETTER, A. J., FROST, J. C., GAUGHAN, J. P., GRAY, G. W., and MOSLEY, A., 1979, *J. Phys. Paris*, **40**, 375.
[87] COLLIN, D., GALLANI. J. L., and MARTINOTY, P., 1986, *Phys. Rev.* A, **34**, 2255.
[88] KELLER, E. N., 1989, *Macromolecules*, **22**, 4597.
[89] INDEKEU, J. O., and NIHAT BERKER, A., 1986, *Phys. Rev.* A, **33**, 1158.
[90] TINH, N. H., ACHARD, M. F., HARDOUIN, F., MAUZAC, M., RICHARD, H., and SIGAUD, G., 1990, *Liq. Crystals*, **7**, 385.
[91] KELLER, P., 1985, *Macromolecules*, **18**, 2337.
[92] KELLER, P., 1985, *Makromolek. Chem. rap. Commun.*, **6**, 707.
[93] KELLER, P., 1988, *Molec. Crystals Liq. Crystals*, **157**, 193.
[94] MEYER, R. B., LIÉBERT, L., STRZELECKI, L., and KELLER, P., 1975, *J. Phys. Lett., Paris*, **36**, L69.
[95] PERSHAN, P. S., 1988, *Structure of Liquid Crystals.* Part I (World Scientific).
[96] GUINIER, A., 1965, *X-ray Diffraction in Crystals, Imperfect Crystals and Amorphous Bodies* (W. H. Freeman and Co.).
[97] HOSEMANN, R., and BAGCHI, S. N., 1962, *Direct Analysis of Diffraction by Matter* (North-Holland Publishing Co.).
[98] NOIREZ, L., KELLER, P., DAVIDSON, P., HARDOUIN, F., and COTTON, J. P., 1988, *J. Phys., Paris*, **49**, 1993.
[99] HARDOUIN, F., MÉRY, S., ACHARD, M. F., MAUZAC, M., DAVIDSON, P., and KELLER, P., 1990, *Liq. Crystals*, **8**, 565.
[100] LEVELUT, A. M., FANG, Y., and DESTRADE, C., 1989, *Liq. Crystals*, **4**, 441.
[101] COMÈS, R., LAMBERT, M., and GUINIER, A., 1970, *Acta crystallogr.*, **A26**, 244.
[102] DOUCET, J., LAMBERT, M., and LEVELUT, A. M., 1971, *J. Phys., Paris*, **32**, C5a-247.
[103] DE GENNES, P. G., *1979, Scaling Concepts in Polymer Physics* (Cornell University Press), Chap. 1.
[104] DE GENNES, P. G., 1983, *J. Phys. Lett., Paris*, **44**, L657.
[105] ENDRES, B. W., EBERT, M., WENDORFF, J. H., RECK, B., and RINGSDORFF, H., 1990, *Liq. Crystals*, **7**, 217.
[106] KÜHNPAST, K., SPRINGER, J., SCHEROWSKY, G., and DAVIDSON, P., *Liq. Crystals* (to be submitted).
[107] LEVELUT, A. M., 1976, *J. Phys., Paris*, **37**, C3-51.
[108] HARBURN, G., TAYLOR, C. A., and WELLBERRY, T. R., 1983, *Atlas of Optical Transforms* (Bell & Hyman).
[109] RENZ, W., and WARNER, M., 1986, *Phys. Rev. Lett.*, **56**, 1268.
[110] DE GENNES, P. G., 1972, *C. r. hebd. Sèanc. Acad. Sci., Paris* B, **275**, 939.
[111] KLÉMAN, M., 1974, *Points, Lignes et Parois* (Les Editions de Physique).
[112] FABRE, P., CASAGRANDE, C., VEYSSIÉ, M., and FINKELMANN, H., 1984, *Phys. Rev. Lett.*, **53**, 993.
[113] RUPP, W., GROSSMANN, H. P., and STOLL, B., 1988, *Liq. Crystals*, **3**, 583.
[114] HELFRICH, W., 1969, *Phys. Rev. Lett.*, **23**, 372.
[115] BOURRET, A., and DESSEAUX, J., 1978, *Nature Lond.*, **272**, 151.
[116] FRIEDEL, J., 1964, *Dislocations* (Pergamon Press).
[117] ALLAIN, M., 1985, *J. Phys., Paris*, **46**, 225.